1 2 9 0

UNIVERSIDADE Ð COIMBRA

Joana Inês Costa Santos

INFLUENCE OF LIGHT WAVELENGTH ON CELLULAR VIABILITY AFTER PHOTODYNAMIC THERAPY

Dissertação no âmbito do Mestrado em Química Medicinal orientada pelo Doutor Fábio António Schaberle e pela Doutora Lígia Catarina Gomes-da-Silva apresentada ao Departamento de Química da Universidade de Coimbra.

Setembro de 2023

Faculdade de Ciências e Tecnologias
da Universidade de Coimbra

Joana Inês Costa Santos

Dissertação no âmbito do Mestrado em Química Medicinal orientada pelo Doutor Fábio António Schaberle e pela Doutora Lígia Catarina Gomes-da-Silva apresentada ao Departamento de Química da Universidade de Coimbra.

Setembro de 2023

1 2 9 0

UNIVERSIDADE D
COIMBRA

Table of Contents

List of Figures

List of Tables

Definitions and Units

Fluence Rate (Φ)	Emitted radiant energy per unit time [W/cm^2] or [J/s*cm^2]
Fluence or Light Dose (LD)	Optical energy per unit area [J/cm^2]
Time (t)	Irradiation time [s]
Wavenumber ($\tilde{\nu}$)	[cm^{-1}]
Wavelength (λ)	[nm]
Molar Absorption Coefficient (Ɛ)	[M^{-1}cm^{-1}]

Abbreviations

DMEM	Dulbecco's Modified Eagle's Medium
DMSO	Dimethyl sulfoxide
DLI	Dose Light Interval
ER	Endoplasmic Reticulum
GA	Golgi Apparatus
LDC	Light Dose Correction
LED	Light Emitting Diode
ISC	Intersystem Crossing
NRCD	Non-Regulated Cell Death
PBM-T	Photobiomodulation Therapy
PBS	Phosphate Buffer Saline
PDT	Photodynamic Therapy
PI	Propidium Iodide
PS	Photosensitizer
RCD	Regulated Cell Death
ROS	Reactive Oxygen Species
S	Singlet Ground State
T	Triplet State
UV	Ultraviolet

Acknowledgments

Chegando ao fim de mais um capítulo deste percurso cheio de aprendizagem e boas recordações, não posso deixar de expressar gratidão a todas as pessoas que desempenharam um papel fundamental na concretização desta incrível jornada.

Quero agradecer ao meu orientador, Doutor Fábio Schaberle, por toda a partilha de conhecimento e pela constante procura de respostas, mas também novas perguntas, pois a ciência não evolui sem perguntas. Pela ajuda, orientação e motivação para o desenvolvimento deste projeto científico muito ambicioso.

À minha orientadora, Doutora Lígia Gomes-da-Silva, agradecer pela sua disponibilidade e ajuda em todo o processo de aprendizagem e aperfeiçoamento de técnicas, assim como pelo conhecimento transmitido. Pelas discussões científicas, a par do Doutor Fábio, que estimulam o espírito crítico e científico, permitindo a minha evolução académica.

À Luzitin, SA, pela disponibilidade dos fotossensibilizadores, LUZ51P e LUZ10P.

A todo o laboratório de fotomedicina e reatividade, do grupo de química medicinal, que me acolheu e proporcionou um excelente ambiente de trabalho, onde foi possível crescer enquanto cientista, mas também enquanto pessoa. À Mafalda, pelas conversas quase sempre científicas que nos permitiram adquirir espírito de equipa e critico, também agradecer pela disponibilidade no processo. À Doutora Claire, que até dezembro, transmitiu muito conhecimento e foi uma ajuda enorme. À Doutora Ana Mata, que além de imenso conhecimento e paciência para o transmitir, foi uma ajuda preciosa a nível informático.

A todos os amigos e colegas da Licenciatura e Mestrado que tive o prazer de conhecer e que deixaram sempre algo de bom para recordar, obrigada por me terem proporcionado momentos inesquecíveis e que guardarei com carinho ao longo da vida. Um agradecimento especial à minha madrinha de curso, Inês Pardal, mas principalmente à amiga que se tornou, obrigada pelas conversas, conselhos, refeições partilhadas e apoio ao longo desta jornada, ao Evgheni que conheci logo no início do primeiro ano e desde aí foi construída uma amizade para a vida, obrigada pelo apoio, pelos conselhos e por estares sempre ao meu lado. Ao Adelino, que me ajudou imenso neste processo, pelas explicações, mas principalmente pela amizade e pelo apoio, pela maneira de ver tudo de forma positiva e a tirar o bom das coisas menos boas.

Aos meus amigos mais antigos, do tempo da escola, que sempre se mantiveram presentes e disponíveis para longas conversas, como forma de terapia e de aliviar o stress acumulado.

Por fim, à minha família, o grande pilar e o maior incentivo para que todo este percurso fosse possível. Aos meus pais, pela extrema paciência, compreensão, amor, orgulho e valores que me transmitem ao longo da vida. Ao meu irmão, pela sua maluqueira, agradeço por me animar e me ajudar. Aos meus avós, avô Zé e avó Rosa, por me darem amor incondicional e pela transmissão de valores, por sempre querem mais e melhor para mim e pelo incentivo de concorrer à universidade, um sonho comum e cumprido. Obrigada aos meus avós Manuel e Cândida. Aos meus tios, Olga e Fernando obrigada pelo carinho e ao meu primo Santiago, o pequenino da família, que fez perceber que há sempre um tempo para brincar e desanuviar. À minha madrinha, obrigada. A toda a minha família um obrigada por tudo.

Resumo

A terapia fotodinâmica (PDT) combina três elementos: um composto, denominado de fotossensibilizador (PS), que é ativado pela luz, luz e oxigénio molecular. O PS absorve luz, o que induz um estado de energia excitado, em que parte da energia absorvida em excesso é transferida para o oxigénio molecular, produzindo espécies reativas de oxigénio (ROS), particularmente oxigénio singleto, que pode induzir morte celular. Este processo não pode ser considerado independentemente da complexidade do organismo, o que significa que os resultados biológicos causados pela PDT devem ser percebidos, tanto quanto possível, tendo em consideração todas as interações possíveis entre a luz e o PS com compostos endógenos, e as possíveis mudanças induzidas em processos bioquímicos e biológicos normais. O objetivo deste trabalho foi aplicar um protocolo de PDT, ativando um PS com diferentes comprimentos de onda, avaliando a influência da luz na viabilidade celular e as diferenças na utilização de um PS solúvel em água e um hidrofóbico.

De forma a avaliar os resultados da PDT é necessário que o número de fotões absorvidos seja o mesmo para todos os comprimentos de onda utilizados, de acordo com a regra de Kasha. Neste estudo, foram selecionados três LEDs (*light emitting diodes*), que emitem a 415 nm, 505 nm e a 630 nm. Estes LEDs têm a capacidade de ativar, respetivamente, cada pico de absorção das porfirinas. Assim, foram selecionadas duas porfirinas utilizadas anteriormente em PDT, uma denominada LUZ51P, uma molécula hidrofóbica (LogP ca. 3), com capacidade de se acumular em organelos celulares tais como reticulo endoplasmático, complexo de Golgi e/ou mitocôndria, e outra denominada LUZ10P, que é solúvel em água (LogP -1.4) e com localização maioritária na via endocítica. Esta escolha permitiu o estudo de duas moléculas que absorvem nos comprimentos de onda selecionados e que têm diferentes co-localizações nos organelos celulares. Os resultados demonstraram que a viabilidade celular usando a LUZ51P ativada a 415 nm é muito menor do que quando ativada a 630 nm, e que os resultados ativados a 505 nm foram próximos aos obtidos com 415 nm. Usando a molécula LUZ10P, as diferenças para os vários comprimentos de onda foram menos evidentes. Assim, estes resultados sugerem que as diferentes co-localizações dos dois PSs usados têm influência nos resultados de viabilidade celular, mas também influência no processo sinergístico verificado para a luz azul, que aumenta o efeito da PDT em comparação com a luz vermelha. Este processo sinergístico é mais evidente para a LUZ51P em comparação com a LUZ10P.

O tipo de morte celular induzida pela PDT foi avaliado utilizando sondas fluorescentes, sugerindo que a ativação da LUZ51P com luz azul induz morte celular por apoptose, que sugere ser o fator diferencial na viabilidade celular quando comparado com o 630 nm. O processo de indução de apoptose está associado com a libertação do citocromo c, uma proteína que tem na sua estrutura uma porfirina, sugerindo uma possível interação sinergística a 415 nm e 505 nm e menos a 630 nm. Esta hipótese foi testada administrando um inibidor, BAI-1, da cadeia bioquímica relacionada com a libertação do citocromo c, em que os resultados preliminares irradiando a 505 nm e a 630 nm, sugerem um aumento na viabilidade celular comparativamente com os resultados usando apenas o PS para ambos. Os resultados obtidos com o LED 630 nm sugerem que o mecanismo biológico envolvido é mais complexo do que o inicialmente proposto.

Este trabalho permite concluir que a ativação de fotossensibilizadores, nomeadamente porfirinas, com diferentes comprimentos de onda (415, 505 e 630 nm), usando o mesmo número de fotões absorvidos, induz diferentes fototoxicidades. Este efeito também depende da localização sub-celular, sendo mais proeminente para a porfirina com tropismo ER-GA. No geral, estes resultados sugerem que ocorre um processo sinergístico entre o efeito da PDT e a luz a 415 e 505 nm. A ocorrência deste processo sinergístico foi um claro resultado, uma vez que somente com a PDT, e com a condição de ter o mesmo número de fotões absorvidos, a viabilidade celular deveria ser a mesma, independentemente do comprimento de onda.

Abstract

Photodynamic therapy (PDT) combines three elements: a compound, named as photosensitizer (PS), that is activated by light, light and molecular oxygen. The PS absorbs light leading it to an eletronically excited state of energy. Subsequently, part of the excess of the absorbed energy is transferred to molecular oxygen, producing reactive oxygen species (ROS), particularly singlet oxygen, which may induce cell death. This process cannot be considered separately from the organism complexity, meaning that PDT biological outcomes should be understood, as much as possible, accounting all extents of interaction of light and PS with endogenous compounds and the possible changes induced in the normal biochemical and physiological processes. The aim of this work was to perform a PDT protocol activating the PS with light of different wavelengths, evaluating the influence of wavelengths on the cell viability and how a water-soluble and a hydrophobic PS may induce different PDT results.

In order to assess the PDT outcomes using different wavelengths, the number of photons absorbed must be the same for all wavelengths, accordingly to the Kasha's rule. In this sense, we selected three light emitting diodes (LED) emitting at 415 nm, 505 nm and 630 nm. These LEDs have the ability to activate the respective absorption peaks of porphyrins molecules. Thus, two porphyrins previously used in PDT (Photodynamic Therapy) were selected: one hydrophobic molecule (Log P approximately 3) called LUZ51P, with the ability to accumulate in cellular organelles such as endoplasmic reticulum (ER), Golgi apparatus (GA), and/or mitochondria, and another water-soluble (Log P -1.4) called LUZ10P, with predominant localization in the endocytic pathway. The selection of these two porphyrins allows the study of two molecules with different subcellular localizations and that absorb at selected wavelengths. The results showed that the cellular viability using LUZ51P activated at 415 nm is much lower than when its activation was performed at 630 nm; at 505 nm the results were close to that at 415 nm. Using the LUZ10P molecule, the differences between the wavelengths were less evident. Thus, these results suggested that different co-localizations of the two PSs used have an influence on the cell viability, and also have an influence on the synergistic process verified for the blue light. Indeed, the synergistic process observed at 415 nm is more evident for LUZ51P compared to LUZ10P, which exhibits less accumulation in the mitochondria.

The type of cell death induced by PDT was assessed using fluorescent probes, suggesting that activation of LUZ51P with blue light induces cell death by apoptosis.

Apoptosis is associated with cytochrome c release, a protein that has a porphyrin in its structure, suggesting a possible synergistic interaction. This hypothesis was tested giving an inhibitor, BAI-1, of the biochemical chain related to the release of cytochrome c. The preliminary results obtained when irradiating at 505 nm and 630 nm suggest an increase in cell viability compared to the PS alone. The increased cell viability obtained with LUZ51P and BAI-1 at 630 nm were unexpected, which may indicate that the biological mechanism involved is more complex than initially proposed.

This work permit to conclude that activation of photosensitizers, namely porphyrins, with different wavelengths (415, 505 and 630 nm), using the same number of absorbed photons, induces different phototoxicities. This effect is also dependent on the subcellular localization as it was more prominent for the porphyrin with ER-GA tropism. Overall, these results suggest that a synergistic process occurs between the PDT effect and the light at 415 and 505 nm. This is clear because with PDT alone and under the condition of having the same number of absorbed photons, the cell viability should be the same regardless the light wavelength.

1. Introduction

Light in its different spectral regions has been used as a tool in medical treatments due to its various therapeutic effects. One example is Photobiomodulation Therapy (PBM-T), which consists on the use of light to stimulate endogenous compounds.[1,2] Another example combines light and an exogenous compound that is activated by light, denominated Photodynamic Therapy (PDT).[3,2] Both examples use visible light in all its extent ca. 400 nm to 750 nm. In the PDT case, when a deep light penetration is required, the wavelengths used are between 650 nm to 800 nm, where the endogenous chromophores absorb less light in this region. Notwithstanding, blue or green light are also used in PDT and in this case simultaneous stimulation of endogenous compounds might occur, inducing biological responses.[1,4]

There are few, but compelling, evidence in the literature that suggest that PDT protocols using blue light induces additional biological effects compared to those expected only by PDT. A few literature reports comparing PDT using blue (400-450 nm) and red light (600-650 nm) reveal differences in the cell viability between these wavelengths.[5] However, in these studies it was not clear that the same number of absorbed photons was taken into account. This is a requirement to compare biological outcomes using different wavelengths in PDT.

In one report Li and colleagues compared the use of blue light at 450 nm with red light at 630 nm in a PDT protocol using sinoporphyrin sodium (DVDMS). These PDT experiments were carried out in different cancer cell lines, HGC27, MGC803, AGS, and GES-1. It should be noted that in this work, the overlap between the light sources and PS were corrected and the same light dose (6 J/cm^2) was used for both wavelengths. However, they did not use conditions that allow to have the same number of photons absorbed, for the different wavelengths, nor did they correct for the different absorption values. While the latter correction has not been made, the fact that the absorption bands at 450 and 630 nm have identical absortivities (absorbance at 450 nm ca. 0.4 and at 630 nm ca. 0.1), makes the results credible for the biological differences observed for both wavelengths. As a result of this work, the blue light had a higher photodynamic effect than red light, under the same light dose. The red light showed a cell viability of 90% whereas the use of the blue light to activate the PS ends in a reduction of the cell viability of 50%. The mechanism of cell death caused by the blue light mediated PDT was studied, and it was verified that regulated cell death occurs, specifically apoptosis and autophagy.[5] In another study, using only light without an exogenous PS (photobiomodulation protocol), C. Opländer et al. studied the impact of different wavelengths of blue light, from 400 to 480 nm in the cell viability and cell proliferation. The results obtained and published showed that light between the wavelengths 400 to 440 nm, caused cell death, while light with a wavelength at 480 nm resulted in an increase in cell viability, suggesting that light may have opposite effects depending on the wavelength applied.[6]

Considering the above mentioned reports, along others suggestive results in the daily practice of our laboratory in the PDT studies, it was sought to assess the impact of the light wavelength on the PDT outcome. For this, in this master thesis it was evaluated the phototoxicity and the type of cell death after the PS activation with light at 415 nm (blue), 505 nm (green) or 630 nm (red). These studies included a PS soluble in water (LUZ10P) and another hydrophobic (LUZ51P). A fairly comparison is only possible if the activation of the PS in the different wavelengths is made with the same number of photons absorbed, following the Kasha's rule, which is defined as "The emitting electronic level of a given multiplicity is the lowest excited level of that multiplicity".[7,8] The determination of the same number of photons absorbed is made accounting for the overlap of the light source emission and the PS absorption peak and considering the molar absorption coefficient of each absorption peak.[9]

In order to apply the PDT irradiation protocol using LEDs emitting at different wavelengths, it is necessary to have a PS that has the ability to absorb in different wavelengths and specifically in those wavelengths of the LED selected. Examples of PS capable of absorbing light at different wavelengths are porphyrins and their derivates. For this reason, two porphyrins, LUZ51P and LUZ10P were used in this work. These porphyrins were selected due to their distinct physicochemical properties, LUZ51P is a hydrophobic porphyrin and LUZ10P is water-soluble.[10] The fact that they have different solubilities in water makes their intracellular localization to be different.[11] More hydrophobic characteristic gives to the PS the ability to permeate cell membranes by passive diffusion and accumulate in cellular organelles such as mitochondria or ER, while water soluble PSs tend to accumulate in the endocytic pathway.[12] Due to different PS organelle tropism, the biological responses induced by PDT might be different.[13,14]

1.1 Photodynamic Therapy

PDT is a non-invasive and selective clinical procedure used, among other applications, in the treatment of cancer. This technique is based on three components, a PS, light and oxygen, which when used separately have no toxicity, but when combined they produce ROS, which lead to the consequent destruction of tumor cells.[15] PDT is initiated by administration of a PS, a compound that is activated in the presence of light. Following a period after the compound administration, denominated drug-to-light interval (DLI), the PS accumulates in the cells or in the blood vessels. Then, the PS is activated by light with appropriate wavelength, where the selectivity is determined by the illuminated area. Long DLI facilitates the uptake of the PS by the cells, called cellular PDT, while using short DLI will favor the PS to remain in the blood stream, called vascular PDT.[12] PS is ideally irradiated with wavelengths in therapeutic window, between 650 nm and 850 nm, where light is less absorbed by the tissues enhancing the light penetration depth.[16]

The photochemical process underlying PDT starts after the electronic excitation of the PS, which leads to the transition from the singlet ground state, S_0, to the singlet excited state S_n, and then, through a vibrational relaxation process back to the S_1 excited state. It is only in the S_1 state that the photochemical processes of transition to the S0 state occur or to the triplet state T_1 by intersystem crossing (ISC) through isoenergetic electronic spin inversion occur (Figure 1). On T_1 level, three main types of deactivations can occur, such as a transition back to S_0 state by 1) emitting a photon, phosphorescence or 2) through non radiative ISC process, and 3) by energy transfer from T_1 to molecular oxygen, producing singlet oxygen. The latter is known as type II reaction of PDT, which is the dominant reaction of most PS in PDT. Type I reactions of PS with oxygen are based in electron transfer reactions.[3]

Type I reaction is defined by the transfer of an electron to oxygen or adjacent molecules, which causes the formation of radicals (cation or anion). These radicals interact with molecular oxygen, which ultimately results in the production of ROS. Type II reaction is characterized by energy transfer to molecular oxygen ($^3O_2$). This molecule in triplet configuration ($^3O_2$) represents the fundamental state and when energy transfer occurs, the singlet oxygen ($^1O_2$) is formed. Singlet oxygen is a highly reactive species, that is an excited singlet state of molecular oxygen. This species does not have charge and because of that have the capacity to diffuse and penetrate through biological membranes and cytoplasm.[3]

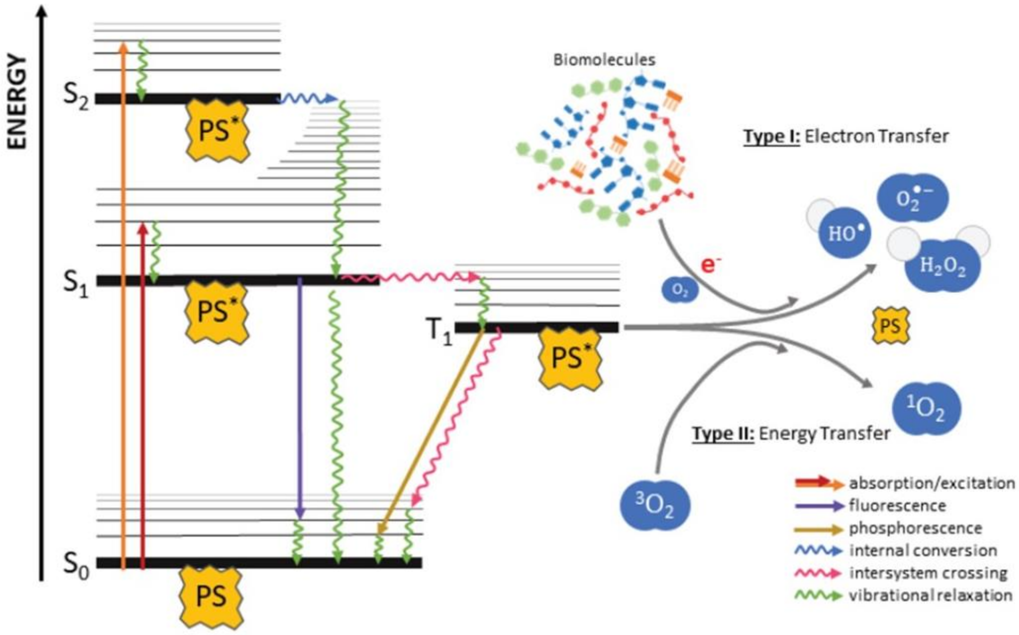

Figure 1. Jablonski Diagram, representing the chemical processes involved in photodynamic therapy (PDT) to produce reactive oxygen species (ROS). Adapted from [17].

The formation of ROS in cells compartments or blood stream can cause cellular damages causing cell death by oxidative stress.[11,18] These processes in cells might produce systemic responses such as local inflammation or immune system stimulation that gives extra advantages for PDT clinical applications.[17]

1.2 Photosensitizers

Most photosensitizers investigated and approved for PDT are porphyrins derivatives, bacteriochlorins and chlorins and phthalocyanines (Figure 2), that have the tetrapyrrolic group as a common structure having a high molar absorption coefficient.[19,16] As the double bounds of tetrapyrrolic structure are reduced, there is a shift of the Q band for longer wavelengths and an increase of the molar absorption coefficients, meaning that the relative intensity of absorption of light increases. Another reason for the use of these compounds is that they have high quantum yields of singlet oxygen production, some also induce type I reaction producing hydroxyl radicals.[16]

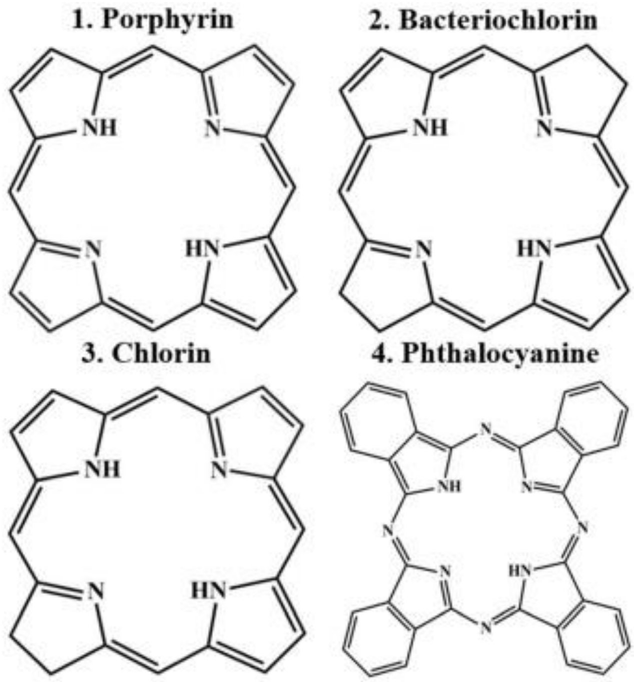

Figure 2. Structures of Photosensitizers. 1. Porphyrin; 2. Bacteriochlorin; 3. Chlorin; 4. Phthalocyanine. Adapted from [20]

An ideal PS should have and meet certain chemical, biological and photophysical requirements.[21,16] It should be easy to synthesize and have high chemical purity and high photostability.[3] In the photophysical aspect, the most important properties are the wavelength where the PS is activated and the quantum yield of the triplet state formation.[19] Then, the PS should have the maximum absorption peak on therapeutic window, where light have higher tissue penetration depth and where the energy of triplet state is high enough to produce singlet oxygen. The localization of PS in sub-cellular organelles is important because accumulation in some intracellular organelles affects the biological response and cell death mechanism. In general, hydrophilic molecules are mostly observed in the endocytic pathway, whereas hydrophobic molecules tend to accumulate in organelles such as endoplasmic reticulum (ER), Golgi apparatus (GA) and/or mitochondria, which are associated with a more lethal effect.[17]

An ideal PS should not have dark toxicity, and during elimination the photoproducts should not cause mutagenic effects or toxic metabolites.[21] After the treatment, the PS should be eliminated by metabolization or excretion, which should be as rapid as possible to minimize the period of photosensitivity and possible side effects (Table 1 presents the most common PSs).[16,20] Most PS are used on anti-cancer treatments, but they can be used for antimicrobial application.[22] Depending on the application, their characteristics vary, as anti-cancer PS should have long wavelength absorption bands and be lipophilic with no charge. Anti-microbial PS should have cationic charges, the wavelength is not so important because microbial infections tend to be superficial.[16]

The first photosensitizer that was clinically approved, was Photofrin, a compound derived from blood porphyrins, which ended in a mixture of dimers and oligomers of Hematoporphyrin. Photofrin or Sodium Porfimer is the PS most used around the world for the treatment of different types of cancer (lung, esophageal, bladder, and etc.), even due to it is limitations, such as skin photosensitivity and small absorbance at longer wavelengths (only up to about 640 nm) that impairs tissue penetration capacity.[23,24] Photofrin is considered as a photosensitizer of 1st generation, and because of the limitations mentioned above, it was further necessary the development of a new generation of photosensitizers with enhanced absorption in the phototherapeutic window.[24,25] Most of the 2nd generation PS were based on chlorins and bacteriochlorins structures. Examples of second-generation PS used on clinic are Temoporfin, Verteporfin and Redaporfin. Verteporfin is a benzoporphyrin derivate, used to treat macular degeneration and has also been re-purposed for oncology trials, including vertebral metastases, breast, and pancreatic cancer.[26] Verteporfin PDT is approved for the treatment of choroidal neovascularization, due to age-related macular degeneration, pathologic myopia, and ocular histoplasmosis syndrome.[26] The photosensitizer Redaporfin, a bacteriochlorin recently synthesized for PDT of solid tumors, is in phase I/II clinical trials for head and neck cancer. In the 3rd generation of PSs, PSs are used bound to antibodies, proteins, peptides, or other molecules. An example is the IRDye700DX (IR700), used as a PS, which has been conjugated with different antibodies, such as human epidermal growth factor receptor 2 (HER2) and epidermal growth factor receptor (EGFR), both completed clinical stages I/II in 2017 and are in phase III clinical trial for head and neck cancer. Cetuximab-IR700, has been approved for the treatment of unresectable locally advanced or recurrent head and neck cancer in Japan (Table 1).[27] As a precursor of the endogenous PS protoporphyrin IX, there is 5-Aminolevulinic acid (5-ALA), which is like a prodrug, that is converted in the cells into protoporphyrin IX. 5-ALA has been investigated for dermatology or topical applications. This PS is used to facilitate the identification of the bladder, malignant brain tumors and other neoplasms and in addition, it is used in the treatment of superficial skin cancer that includes actinic keratosis, squamous cell carcinomas and basal cell carcinoma. ALA can be also applied to the treatment of non-tumoral conditions such as psoriasis.[28]

Table 1. Photosensitizers for PDT that have been approved for clinical. Adapted from [29]

Photosensitizer	Wavelength (nm)	ε (M^{-1} cm^{-1})	Approved clinical application
Porfimer sodium (Photofrin®)	630	3.0E3	Esophageal cancer, Endobronchial cancer, High-Grade Dysplasia in Barrett's Esophagus
Verteporfin (Visudyne®)	689	1.4E4	Age-related macular degeneration (AMD)
Temoporfin/m-THPC (Foscan®)	652	3.0E4	Advanced Head and neck cancer
5-ALA (Levulan®) and its methyl (Metvix®) or benzyl (Benzvix®) ester derivatives*	635	5.0E3	Actinic keratoses
IR700 linked to cetuximab (cetuximab sarotalocan)	690	2.1E5	Head and neck cancer

* These molecules are pro-drugs of the photosensitizing agent, PpIX.

The two PSs used in this work were LUZ51P and LUZ10P, which have different physical and chemical characteristics. The biological effects produced by PDT are influenced by the localization of PSs in the cells. The subcellular localization is influenced by the chemical characteristics of PSs, but also by the concentration of PS that is administrated and by the incubation time. The intracellular tropism of the PSs can be predicted by the hydrophobicity of the compounds. Through images kindly provided by Dr. Lígia Gomes da Silva, it is known that the LUZ10P and LUZ51P have different co-localizations. While porphyrin LUZ10P being more hydrophilic, tends to be observed in acidic vesicles, as shown in Figure 3A. In contrast, LUZ51P is a hydrophobic compound that significantly accumulates in the endoplasmic reticulum and/or Golgi apparatus compartments with lower accumulation at the mitochondria, as can see in Figure 3B.

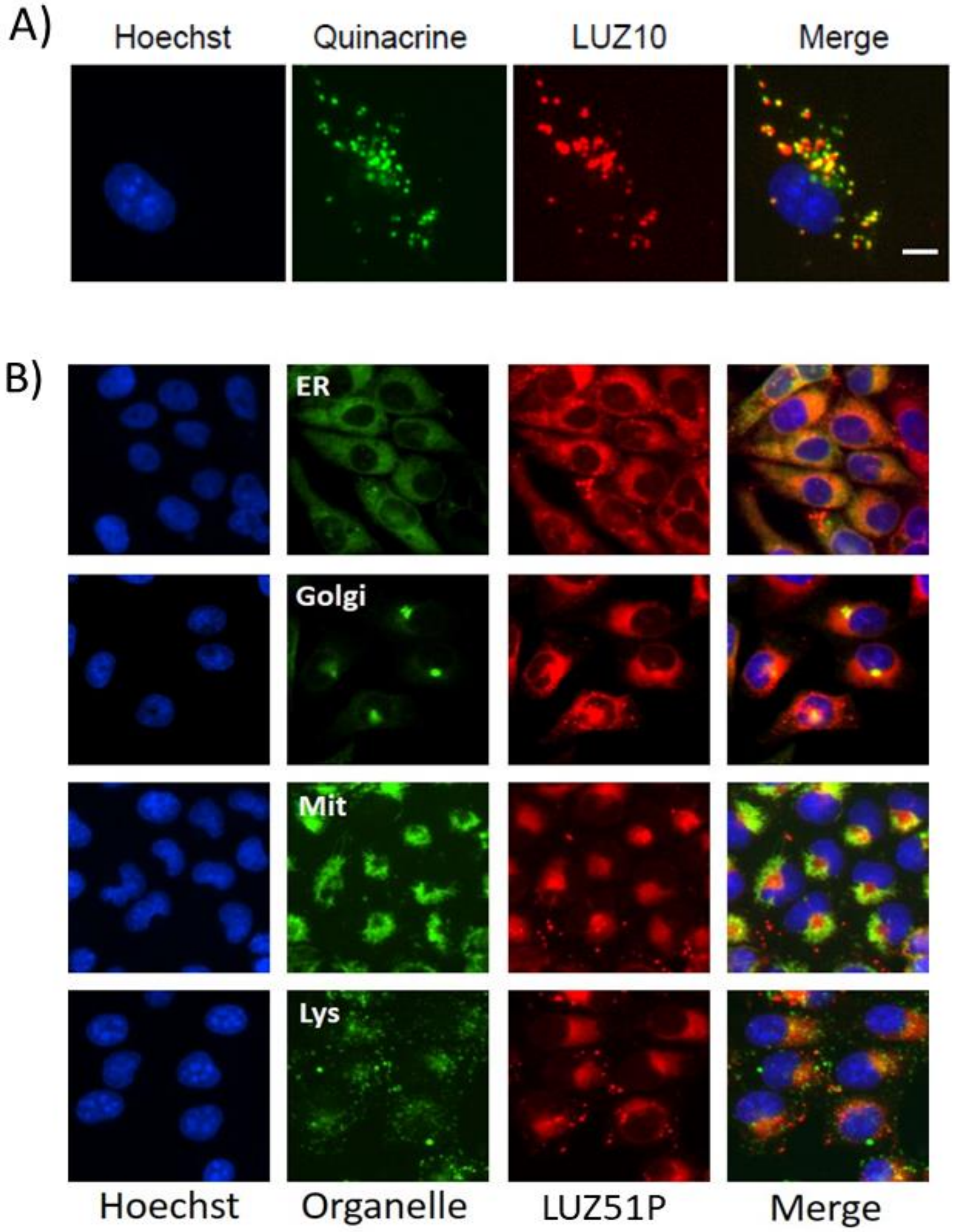

Figure 3. Co-localization of the photosensitizers A) LUZ10P with acidic vesicles and B) LUZ51P with the ER-GA compartments.

1.3 Main Mechanism of Cell death in PDT

In the PDT process, in particular, during tumor cell irradiation, photochemical reactions occur, that lead to the production of different ROS, which in turn cause cell death by different pathways, including regulated cell death (RCD) and non-regulated cell death (NRCD). Different cell death types can be classified through morphology, functional aspects, enzyme involvement or immune characteristics. At the morphological level, it can be classified as necrosis, apoptosis, autophagy, or death related to mitosis processes. At the functional level, it can be classified as programmed or accidental death and pathological or physiological death. In the involvement of enzymes, can be subdivided between the involvement of nucleases or caspases.[30]

RCD includes a large variety of cell death modalities that are regulated by various signal pathways of high complexity. In contrast, NRCD is an uncontrolled and quick form of death, typically called as necrosis. The most studied mechanisms of cell death in PDT are necrosis, autophagy, and apoptosis. However, other modes of cell death have emerging in the last decade. Typically, when high dose light and/or high concentration of PS are used, necrosis is caused, while lower photodamage activates RCD.[31] This means that at the surface of the tumor where is a high photodamage owing to a higher photon flux, necrosis is often observed. On the contrary, when the tumor cells are in deeper regions, they die mainly through regulated cell death, such as apoptosis.[32]

Necrosis is an accidental pathway of cell death, and it is characterized by autolysis after exposure to physiochemical stimulus. Morphologically, it is described by a gain in cell volume, cytoplasmatic granulation and/or cellular swelling and breakdown, followed by the release of cell contents and pro-inflammatory molecules.[31]

Autophagy is a process that acts in two different ways, as a cell death mechanism or a pro-survival mechanism, which depends on the level of the photodamage that is induced to the target cells. Autophagy is a catabolic process that relies on the sequestration of cell components to subsequent degradation in the lysosomes. Autophagy is initiated by stress factors, such as nutrient deprivation or damaged organelles or in physiological conditions such as during embryogenesis and cellular differentiation.[33]

In order to occur autophagy, it is necessary the formation of autophagosomes, which are double-layer vesicles involving the damaged material, to isolate it from the cytoplasm, and subsequently occur fusion with lysosomes, which form the autolysosome. In the autolysosome, there are two processes, namely the degradation of damaged material by the lysosomal hydrolases and the consequent removal of these materials. Additionally, the process of nutrient recycling occurs, wherein the nutrients are reused for cell processes.

1.3.1 Apoptosis

Apoptosis is a cellular physiological process that functions in maintaining cellular homeostasis and regulating embryonic development. It can also be considered a defense mechanism against infected cells, namely with viruses or other intracellular pathogens.[34] To initiate the apoptotic process, it is necessary to have a suicide stimulus, endogenous or exogenous, such as DNA mutations, protein oxidation. Cell death mediated by apoptosis is defined by morphological changes such as cell blebbing, chromatin condensation, DNA fragmentation, changes in plasma membrane and the formation of apoptotic bodies, which will be phagocytosed, thus avoiding an inflammatory response. Apoptosis is subdivided into two pathways, extrinsic or death receptor and intrinsic or mitochondrial apoptosis.[35,33]

The intrinsic pathway is the apoptotic pathway more often discussed in the context of PDT.[36] This via is characterized by mitochondrial dysfunction that includes the output of cytochrome c to cytosol and consequent activation of caspases, that consequently provoke membrane blebbing, cell shrinkage and DNA fragmentation. The principal step is irreversible mitochondrial outer membrane permeabilization (MOMP), which is regulated by BCL-2 family.[37] BCL-2 family is subdivided in pro and anti-apoptotic members. Pro-apoptotic members include BAX, BAK proteins which promote the release of cytochrome c and others mitochondrial proteins into the cytosol, through the selective formation of pores in the mitochondrial outer membrane. On the other hand, BCL-2, BCL-xL are anti-apoptotic proteins that promote cell survival by sequestering or neutralizing pro-apoptotic proteins.[31]

MOMP promotes the irreversible cytosolic release of apoptogenic factors, such as cytochrome c, from the inner membrane of mitochondria to cytosol.[38] The release of cytochrome c is preceded by the disruption of its interaction with an inner mitochondrial membrane-specific phospholipid cardiolipin (CL). During apoptosis, conformational changes in the tertiary and secondary structure of cytochrome c, owing to breaks in binding between the heme group of cytochrome c and an amino acid of CL, or replacement of amino acid residues, which lead to a significant increase in the peroxidation activity of cardiolipin.[39,40] In the cytosol, cytochrome c binds to other proteins, namely Apaf-1, pro-caspase-9, dATP/ATP and other proteins, forming the apoptosome. After the formation of apoptosome, a family of cysteine protein enzymes, called caspases, are activated. Initially, pro-caspase-9 is cleaved into the active caspase 9. The latter activates the caspases cascade that ends in the activation of the effector caspases 3 and 7, which executed cell death through the cleavage of a wide range of other cellular proteins (Figure 4).

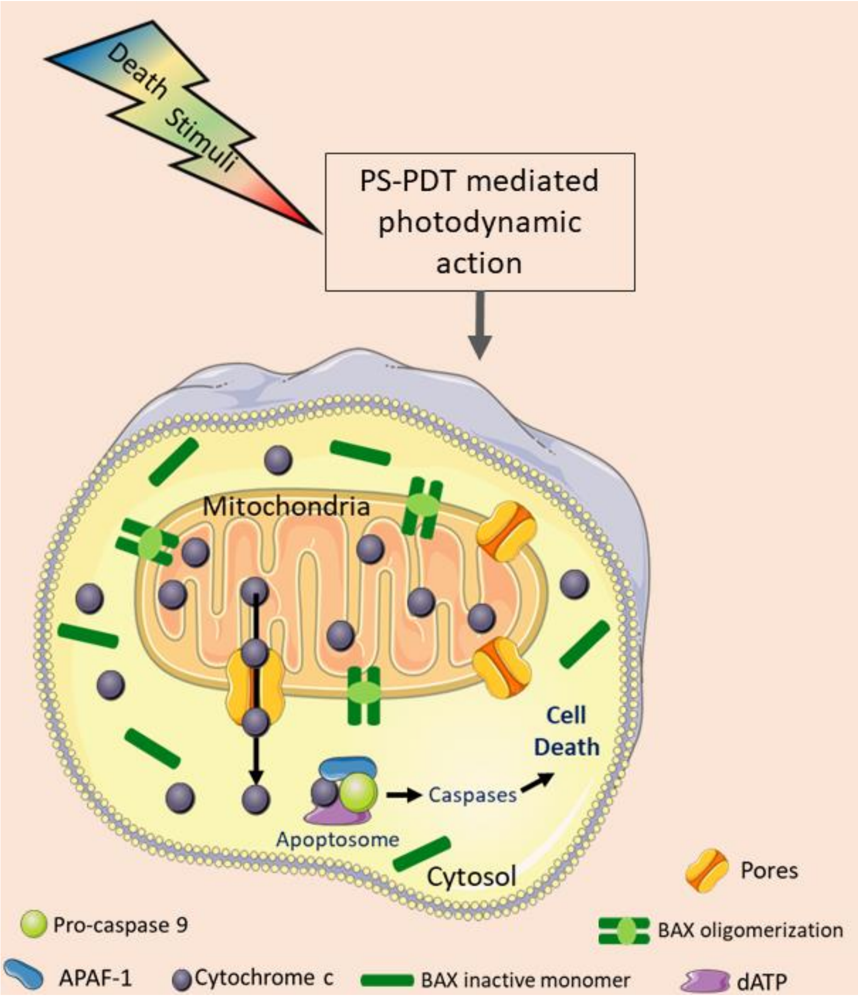

Figure 4. Representation of the intrinsic pathway of apoptosis. The Figure was partly generated using Servier Medical Art, provided by Servier, licensed under a Creative Commons Attribution 3.0 unported license.

The extrinsic pathway is also denominated the cell death receptor pathway as it is activated by members of the Tumor Necrosis Factor (TNF) receptor gene superfamily. The activation of these receptors is made from intracytoplasmic region, which contains adaptor proteins that interact with the pro-caspase 8. When activated, it recruits adaptor molecules that cleaved pro caspase 8, into caspase 8.[41] The latter triggers the activation of the caspase cascade which, similar to the intrinsic pathway, culminates in the activation of the effector caspases, 3 and 7.

1.4 Photobiomodulation Therapy and Endogenous Chromophores

Photobiomodulation therapy (PBM-T) is a technique that uses only light for therapeutic purposes. While in PDT there is an exogenous compound that is activated by light and produce a therapeutic effect, in PBM-T the light interacts with endogenous compounds, which produces therapy effects.[2,1]

The light from visible range to NIR zone, 400 nm to 1100 nm, has photochemical and photophysical effects capable of modulating biological processes, such as cell proliferation, inflammatory signaling and mitochondrial functions. These biological effects are likely mediated through interactions of light with endogenous chromophores.[1] The most studied wavelengths are in the NIR and red light, 600-1100 nm, due to their anti-inflammatory effects and enhanced DNA repair activity and proliferation.[42,4] The use of light at 400 nm and below has not been extensively studied due to the fact that the therapeutic margin is not well defined. In addition, the blue light has less penetration depth on tissues, compared with red light. Due to this limitation, blue light has been studied mainly to reduce inflammation on the surface of tissues, to promote wound healing and to limit bacterial growth.[43] The green light is being used for the stimulation of angiogenesis and myofibroblast differentiation and holds anti-inflammatory effects as well.[42]

The endogenous molecules that have the ability to absorb the light used in these therapies are called endogenous chromophores. These molecules, when irradiated tend to suffer alterations (e.g. photochemical modification [44]) causing endogenous reaction. Examples of these chromophores are hemoglobin, myoglobin, cytochrome c, flavins, flavoproteins and porphyrins (Table 2).[44,45] Cells have several chromophores capable of absorbing blue and green light. Examples of these compounds are chromophores located in mitochondria and with a role in the electron transport chain, such as the P450 family or complex I that have a greater tendency to absorb in the ultraviolet (UV) and blue light, from 390 to 460 nm, or the complex III that have the capacity to absorb green light.[46]

Table 2. Absorption of the main endogenous biomolecules. Adapted from [42]

Endogenous Biomolecules	Optical Absorption (nm)
Vitamin E	200 – 320
Heme Group	200 – 650
Vitamin B12	240 – 600
Flavin	300 – 550
Melanin	300 – 800
Lipofuscin	300 – 500
Opsins	400 – 680

Cytochrome c is being pointed as an important player of the therapeutic effects of PBM-T. It is a small mitochondrial protein, water-soluble, with approximately 100 amino acid residues and contains a heme as a prosthetic group (Figure 5).[40] This protein belongs to c type cytochrome family, which have fundamental functions in life sustainment and cell death, that means, it has vital role on mitochondrial electron transport chain and on apoptosis, respectively. On cells, the cytochrome c is in the intermembrane space of mitochondria, acting between inner and outer mitochondrial membranes. Due to its highly positive charge, cytochrome c is associated with negatively charged phospholipids, especially CL.[47] It is at this local of the inner membrane that cytochrome c is involved in the transfer of electrons between the complex III (reductase cytochrome c) and complex IV (cytochrome c oxidase). Cytochrome c oxidase (COX) contains two heme and two copper redox centres.[47]

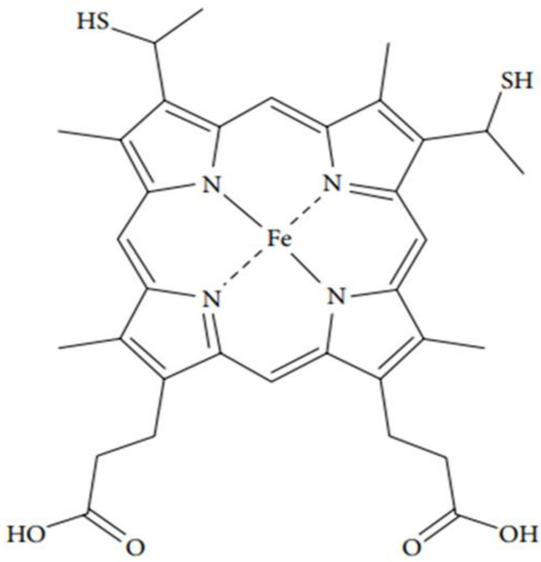

Figure 5. Structure of heme c, the prosthetic group of cytochrome c. Adapted from [48].

Overall, the main objective of this project was to verify the effect caused on cell viability, when using different wavelengths and PSs with different co-localizations. For this, the two selected PSs, LUZ51P and LUZ10P, were both activated with three different wavelengths (415, 505 and 630 nm), accounting for the same number of photons absorbed. The PDT biological outcomes were assessed through the cellular viability/ phototoxicity and by identifying the type of cell death.

2. Material and Methods:

2.1 Reagents

The culture medium used in in vitro studies was Dulbecco's Modified Eagle's Medium-high glucose (DMEM), acquired from the company Sigma-Aldrich. This culture medium consists of a concentration of 4500 mg/L of glucose and L-glutamine and red phenol. The culture medium used in the irradiation process, was RPMI-1640 purchased from Sigma-Aldrich, which is composed of L-glutamine, but without red phenol. Both culture medium, DMEM and RPMI, were supplemented with sodium bicarbonate and 4-(2-hydroxyethyl) piperazine-1-ethanesulfonic acid buffer (HEPES), acquired in Sigma-Aldrich, as well as with 10% of fetal bovine serum (FBS), purchased from Gibco and with 1% of penicillin-streptomycin, acquired in Sigma-Aldrich.

Trypsin-EDTA solution (10x), dimethyl sulfoxide (DMSO), trypan blue, propidium iodide (PI) and Alamar blue (resazurin were obtained from Sigma-Aldrich. Hoechst 33342 was purchased from Life Technologies. The inhibitor BAI-1 was acquired from TargetMol.

Photosensitizers LUZ51P and LUZ10P were kindly provide by LUZITIN SA.

2.2 Equipment:

The weights of the PS LUZ51P, for the calculation of the molar absorption coefficient were made on the calibrated analytical balance, Kern ALJ 220-5DNM. The absorption spectra of the PSs were recorded in the UV-Visible recording spectrophotometer, Shimadzu, using standard quartz cuvettes with an optical path of 1 cm.

All the procedures involved in the in vitro studies, from the preparation of solutions and reagents to the execution of the protocols, were carried out in the flow chamber, Thermo Scientific MSC Advantage. The light sources used were light-emitting diodes (LEDs), with emission at 415 nm and 505 nm, Thorlabs, and at 630 nm from Edmund

Optics. The fluence rate values of the LEDs was measured with a Coherent LaserCheck power meter.

The fluorescence emission of resazurin/resorufin ($\lambda_{excitation}$ = 528/20 nm and $\lambda_{emission}$ = 590/35 nm) was obtained using Synergy HT Multi-Mode Microplate Reader (BioTek). To observe the cells morphology and the dyes (Hoechst 33342 and propidium iodide) used to mark the cells, it was used an Olympus CKX41 inverted microscope equipped with an Olympus U-RFLT50 power supply unit.

2.3 Studies in Solution

2.3.1 Determination of the Molar Absorption Coefficient

LUZ51P porphyrin solutions were prepared in DMSO, with a concentration of 0.5 mM. For that, 0.88 mg and 1.3 mg of compound with a molar mass of 595.59 g/mol were weighed, and 2.96 mL and 4.36 mL, respectively, of DMSO were added to get a final concentration of 0.5 mM. To avoid precipitates or aggregates, the solutions were mixed using vortex and ultrasound bath.

The determination of the molar absorption coefficients of LUZ51P compound, was made by weighing two masses and successive dilutions from stock solutions. Through absorption spectra, the absorbances values were obtained as a function of the concentration of solutions. Having these data, absorbance and concentration, a linear fit was made, where the slope of the regression line corresponds to the molar absorption coefficient in accordance with the Beer-Lambert Law equation (1).

2.3.2 Preparation of Solutions

The studies were initiated by preparing a stock solution of LUZ51P (Figure 6A). After the preparation of the solution the absorption spectrum was obtained, and the concentration of stock solution was calculated using the Beer-Lambert Law equation (1) and the molar absorption coefficient determined in this work.

$$A\ (\lambda) = \ \varepsilon\ (\lambda)\ l\ c \tag{1}$$

Where A(λ) corresponds to the peak absorbance at the desired wavelength, ε corresponds to molar absorbance coefficient ($M^{-1}cm^{-1}$), l corresponds to optical path length (cm) and c is the concentration of solution (M).

From the initial solution, with a concentration of 1.77 mM, a diluted solution was prepared, in which 85 µL of the initial solution was diluted in 2915 µL of DMSO. The absorbance spectrum was obtained, and the concentration was calculated, having a final concentration of 0.058 mM. Both solutions were stored at -4 ºC and protected from light with aluminum foil. The solutions to be added to the cells were prepared by diluting the solution in culture medium (DMEM), to obtain the necessary concentrations.

In PDT studies, due to the differences in the uptake of LUZ51P and LUZ10P, different concentrations of each PS were used. Then, an initial solution of LUZ10P (Figure 6B) was prepared in 1 mL of Phosphate Buffer Saline (PBS). The LUZ10P solution was prepared in the day of the experiment to avoid chemical and photochemical instabilities in PBS.

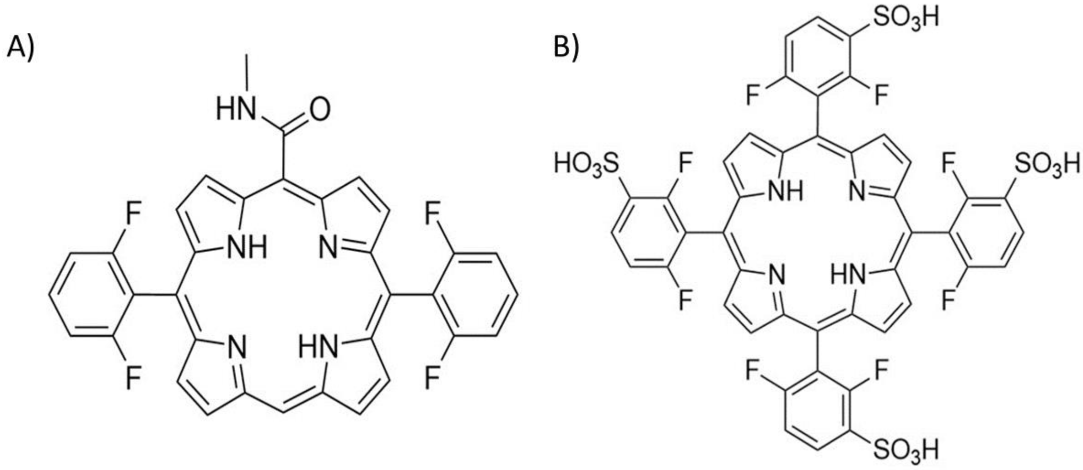

Figure 6. Structure of the porphyrin photosensitizers A) LUZ51P and B) LUZ10P

2.3.3 Singlet Oxygen Quantification

To evaluate of the production of singlet oxygen, using 0.1 µM of LUZ51P, a selective fluorescent probe for the singlet oxygen was used. The probe used was the singlet oxygen sensor green (SOG), which initially has a fluorescence peak in the blue range, with excitation peak at 371 and 393 nm and an emission peak at 395 and 416 nm. When there is the presence of singlet oxygen, SOG is oxidized and emits green fluorescence, with excitation peak at 504 nm and emission peak at 525 nm.[49]

First, 33 µL of methanol were added to 110 µg of SOG, to obtain a solution of 5 mM. From this solution four solutions were prepared with 1 mL of methanol or RPMI, two solutions with 25 µM of SOG and the other two solutions with 25 µM of SOG and 1µM of LUZ51P. Afterwards, the solutions were transfer to three plates of 96 wells, one for each LED, being used the following LEDs conditions: 415 nm LED (Φ = 0.174 mW/cm^2 and LD between 0 to 1.6 J/cm^2), 505 nm LED (Φ = 2.2 mW/cm^2 and LD between 0 to 3.2 J/cm^2) and 630 nm LED (Φ = 13.6 mW/cm^2 and LD between 0 to 54.4 J/cm^2). After each irradiation time, fluorescence signals for the SOG and SOG + LUZ51P were measured, and the SOG signal was obtained by the subtraction between the SOG + LUZ51P and SOG signal.

2.4 *In vitro* studies

2.4.1 Cells Culture

The cell line used in this work was 4T1 line, breast cancer cells derived from the mammary gland tissue of Balb/c mice. The cells were maintained in culture medium, DMEM, in 75 cm^2 sterile flasks. Cells were maintained in an incubator that was at 37°C with 5% of CO_2. After an incubation period of 2 or 3 days, the confluence of cells in culture flasks was obtained, and it was necessary to pass cells. This procedure involves washing the flask with 5 mL of PBS and an incubation period of 6 min with 3 mL of trypsin. After that period, the cells were homogenized, and a small portion of this volume was left with 15 mL of DMEM, to have a new cell growth.

2.4.2 Cytotoxicity

Cytotoxicity studies were carried out with the objective of evaluating the toxicity of the compound in the dark, in order to select concentrations that do not present toxicity in the absence of light. Four days study, with an incubation time of 24 h, were carried out to assess cytotoxicity. On the first day, 6000 cells were seeded per well in 96 wells plates and grown overnight. After attaching, cells were incubated with LUZ51P solutions at different concentrations, varying between 0.0125 µM to 0.4 µM. After an incubation period of 24 h, the cells were washed twice with PBS solution, to remove the compound that was not internalized by the cells and DMEM was added.

Cell viability was evaluated 24 h after, using the Alamar Blue method. For this, 0.01 mg/mL of resazurin diluted in medium was added to cells and to 3 wells without cells which served as the basal control of the fluorescence of the initial stock of resazurin. The cells were then placed in the incubator and after 1 h, the metabolization of resazurin, a non-fluorescent and blue compound, to resorufin, a fluorescent and pink compound, by live cells began to be noticed. Finally, the data was analyzed considering that the untreated cells have an metabolization of resazurin that corresponds to 100% of cell viability.

2.4.3 Phototoxicity

Phototoxicity assays were run with the objective of evaluating the influence of different wavelengths on cell viability (Figure 7). On the first day, 6000 cells were seeded per well in 96 wells plates and grown overnight. After attaching, cells were incubated with LUZ51P solutions with different concentrations, varying between 12.5 and 100 nM, or with LUZ10P solutions with concentrations varying between 10 and 50 µM. Twenty-four hours later, cells were washed twice with PBS solution, in order to remove the compound that was not internalized by the cells and RPMI without red phenol was added. The plates were irradiated with three different LEDs, 415 nm blue LED, 505 nm green LED and 630 nm red LED, during 40 min, with the conditions described in section 3. After the irradiation, RPMI was removed and DMEM was added, cell viability was evaluated 24 h post-irradiation by a resazurin assay as mentioned above.

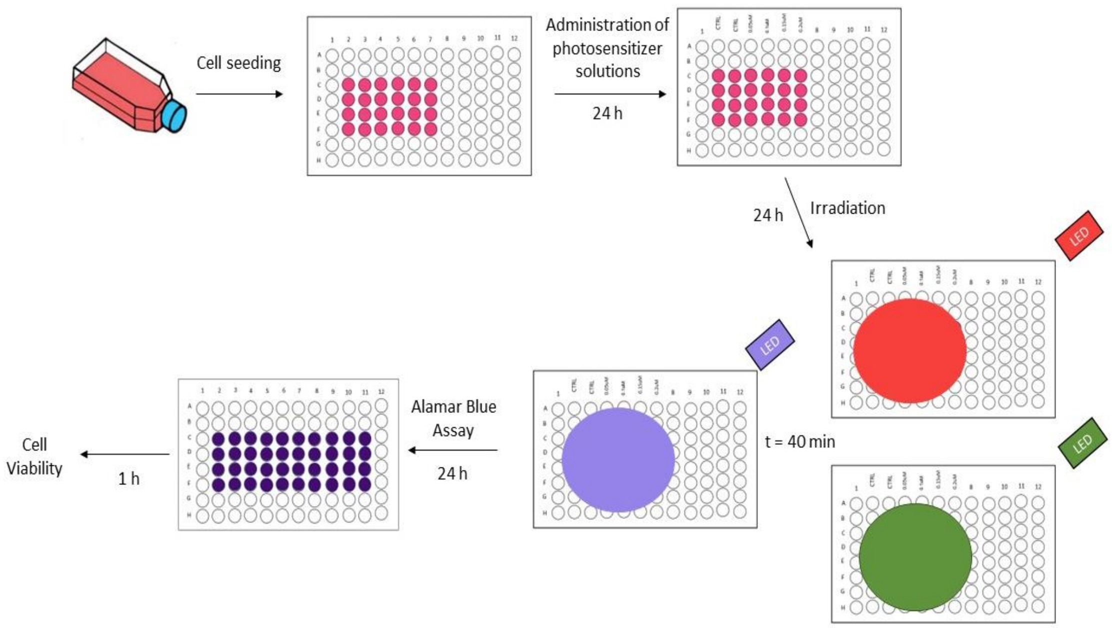

Figure 7. Scheme of *in vitro* assays.

2.4.4 Fluorescence Microscopy

40 000 4T1 cancer cells were seeded in 24-wells plates at a final volume of 500 µL of DMEM. After 24 hours, LUZ51P was added with the final concentrations of 12.5, 25.0 and 50.0 nM, and 24 hours later, cells were washed followed by irradiation with three different wavelengths, 415, 505 and 630 nm, with the conditions previous described. After 3, 6 and 24 hours the cells were incubated with Hoechst, in the ratio of 1:5000, and propidium iodide (1 mg/mL), 20 minutes before each timepoint. Afterwards, cells were analyzed by fluorescence microscopy using a 20x objective.

2.4.5 Cytochrome c inhibitor (BAI-1)

In order to prepare the inhibitor solution, BAI-1 (Figure 8), 5 mg were diluted in 2 ml of DMSO, resulting in a solution with a concentration of 5.35 mM. From this solution, a diluted solution was prepared, with a concentration of 1 mM. For the *in vitro* studies using the BAI-1 inhibitor, the entire process of preparing the plates for phototoxicity studies was repeated, except that on the third day of the experiment, 2.5 hours before irradiating the cells with the various wavelengths, 150 µL BAI-1 solution was added to the wells containing 150 µL of LUZ51P. After an incubation of 2.5 hours, the wells were washed with PBS and fresh BAI-1 solution prepared in RPMI was added, which was followed by cells irradiation as mentioned in section 2.4.3.

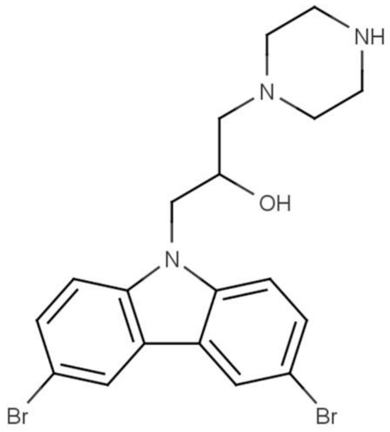

Figure 8. Structure of BAI-1.

2.4.6 Statistical Analysis

Dark toxicity and phototoxicity data were represented as mean ± SEM, for three individual experiments, n=3, with triplicate wells for each concentration, as well as the control group. Two-way ANOVA calculations was performed to compare the means of each group for the different LEDs.

3. Determination of the Number of Photons Absorbed

In PDT, according to the Kasha's rule, the important parameter in the generation of singlet oxygen is the number of photons absorbed and not their energies, since after excitation to higher singlet excited states the PS deactivates fast and non-radiatively to the S_1 excited state, before undergoing to the process of transferring energy to the oxygen. This is of most importance when comparing PDT biological outcomes using different wavelengths. Thus, the determination of the number of photons absorbed were made in two steps. First, it was calculated a correction factor for the overlap between the LED emission spectrum and the absorption peak of the PS and second, it was determined the same number of photons absorbed considering the absorption coefficient.

A LED is characterized by a broad emission band (ca. 50 nm), while a LASER is characterized by a narrow emission band (ca. 1 nm). Thus, since the LED has an emission spectrum and the PS has an absorption spectrum, it was necessary to proceed with the determination of the overlapping region between them.[9] This overlap translates to the actual number of photons absorbed when using a broadband light source. With this procedure a light dose correction (LDC) can be calculated, which makes it possible to make the equivalence between a LED and a LASER emitting in the peak of absorption of the absorber. This process can be observed in Figure 9 where the number of photons that are effectively absorbed by LUZ51P when using the LED at 415 nm are within the overlap area.

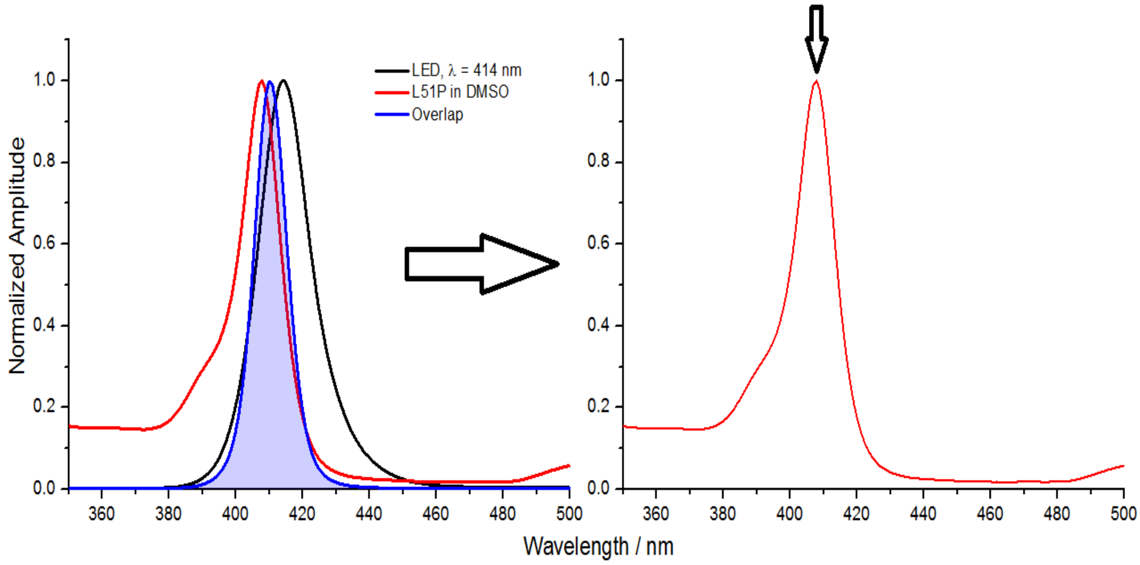

Figure 9. Representation of the equivalence process, in which in the graph on the left is the emission spectrum of the LED 414 nm (black), absorption spectra of the LUZ51P (red) and corresponding overlap of the two spectra (blue). The LDC correction can be interpreted as if the photons absorbed, represented in the overlap, were emitted by a LASER light source at the absorption peak (figure in the right)

The LDC factor is determined by the ratio between the number of photons emitted by the light source and the number of photons absorbed by the PS if a LASER source was used. To perform the LDC determination, it is necessary to have: i) the absorption spectrum data of the PS (Abs), ii) the emission spectrum of the light source (LED) in function of the wavenumber ($\tilde{\nu}$) and the value of the wavenumber ($\tilde{\nu}_{peak}$) corresponding to the maximum of absorption (Abs($\tilde{\nu}_{peak}$)) value of PS, as illustrated in the Table 3.

Table 3. Example of a file containing the data required to calculate the LDC. *Corresponds to the calculation of the number of photos normalized

Wavenumber (ṽ)	**LUZ51P Absorption (Abs)**	**LED Emission (LED)**	**Number of Photons ***
28571,43	0,01465	1,35E-6	1,57E-12
28309,77	0,01464	1,86E-6	2,18E-12
28052,85	0,01513	2,41E-6	2,94E-12
27800,56	0,01653	3,04E-6	4,09E-12
27552,76	0,01936	4,88E-6	7,73E-12
27309,35	0,02373	9,41E-6	1,83E-11
27070,19	0,02837	1,86E-5	4,35E-11
26835,19	0,03252	3,68E-5	9,91E-11
26604,24	0,03808	7,24E-5	2,28E-10
26377,22	0,04904	1,37E-4	5,54E-10
…	…	…	…

First, the sum of the values of the LED emission spectrum is normalized for each value of the wavenumber, that is, the sum is equal to 1, equation 2. After normalization, the number of photons is calculated, following equation 3. The number of photons corresponds to the sum of the normalized emission spectrum of the LED in function of the 'wave number' times the light absorbed by the PS.

$$\sum LED(\tilde{v}) = 1 \tag{2}$$

$$Number\ of\ Photons = \sum \frac{LED(\tilde{v})}{\tilde{v}}\ (1 - 10^{-A(\tilde{v})}) \tag{3}$$

Then, the value of LDC can be obtained using equation 4, where A_{peak} and $\tilde{v}_{peak}$ are the absorption and the wavenumber at the peak of absorption, respectively.

$$LDC = \frac{Number\ of Photons}{\frac{1}{\tilde{v}_{peak}}(1-10^{-A_{peak}})} \tag{4}$$

For this example, using the data from Table 3 to calculate the LDC factor, and by overlapping the spectra (Figure 10), the value of LDC obtained was 0.53, meaning that only 53% of the light is absorbed by the PS when using this LED.

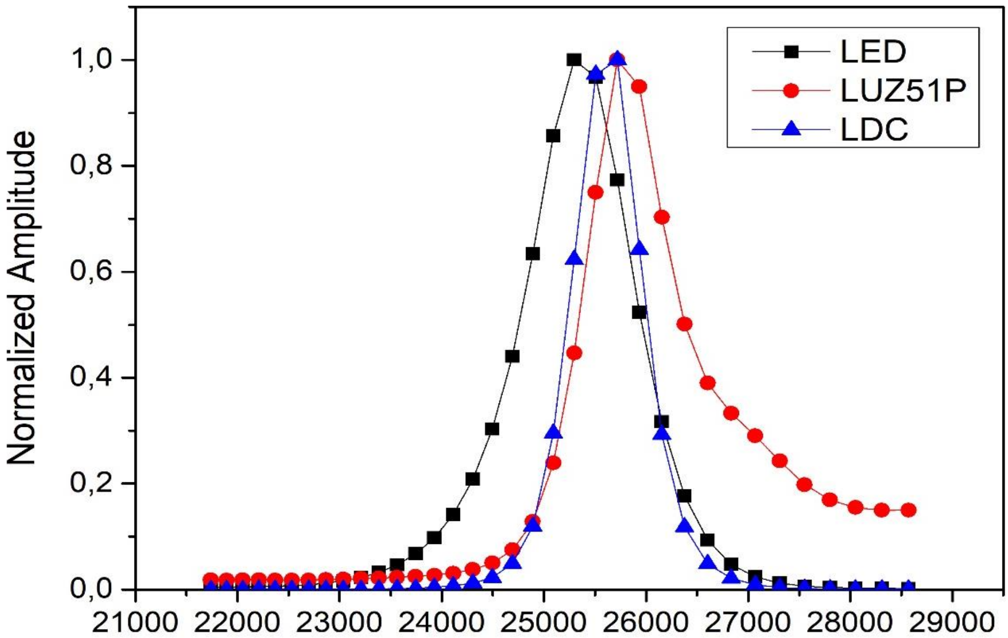

Figure 10. Representation of LDC calculation, with the emission spectrum of the LED (black), absorption spectrum of the LUZ51P (red) and corresponding photons absorbed (blue).

In order to be able to compare the PDT results using different wavelengths, it was necessary to determine the initial number of photons for each wavelength, aiming to have the same number of photons absorbed. The calculation of the number of photons absorbed was made using the Beer-Lambert law, equation 5.

$$I_{abs} = I_0\,(1 - 10^{-A}) \tag{5}$$

Considering, that the intensity corresponds to the number of photons per unit of second and area, it is possible to correlate the intensity with the fluence rate, as demonstrated in equation 6.

$$I = \frac{1}{Area}\frac{dn}{dt} = \frac{\Phi}{E_{h\,v}}\left[\frac{J}{s\ cm^2\ J}\right] = Photons\ \left[\frac{1}{s\ cm^2}\right] \tag{6}$$

$$\frac{dn_{abs}}{dt} = \frac{dn_0}{dt}\left(1 - 10^{-A(\tilde{v})}\right) \approx \frac{dn_{abs}}{dt} = \frac{dn_0}{dt}\ A(\tilde{v}) \tag{7}$$

The equation (6) provides the relation between the fluence rate and the number of emitted photons, and the equation (7) demonstrates the relation between the number of photons absorbed and the molar absorptivity coefficient (A). This relation is possible as according to the Taylor series approximation, the term $(1 - 10^{-A})$ can be approximated to the value of the absorbance (A), becoming a linear equation. This approximation is possible when the value of A is much lower than 0.1. This is true for absorption of PS in the cell, considering that the optical path length of the cell is of the order of micrometers, and the concentration of PS in the cells should be low. Through earlier PDT experiments the number of initial photons using the LED at 505 nm, to cause decrease in cell viability, was determined as $\frac{dn_0}{dt} = 3.0\ \times 10^{15}$. Taking into account that the main premise of this work is that the number of photons absorbed must be the same for all three LEDs and using the LED at 505 nm as a reference, it was calculated the initial number of photons for the other two LEDs, 415 and 630 nm, following the equation (8) and (9).

$$\frac{dn_{abs}}{dt} = 3.0 \times 10^{15}\ \times\ \mathcal{E}\,(505\,nm) \tag{8}$$

$$\frac{dn_{abs}}{dt} = \frac{dn_0}{dt} \times\ \mathcal{E}\,(415\,nm) \tag{9}$$

The ratio between the equation 8 and 9 was made to calculate the initial photon number for the LED at 415 nm, as demonstrated by equation 10.

$$1 = \frac{3.0 \times 10^{15} \times \mathcal{E}\,(505\ \mathrm{nm})}{\frac{\mathrm{dn_0}}{\mathrm{dt}} \times \mathcal{E}\,(415\ \mathrm{nm})} \tag{10}$$

The same procedure was used to calculate the initial photon value for the LED at 630 nm. Therefore, having the value of the number of photons absorbed, $\frac{dn_0}{dt}$ for the three LEDs, these values were used through the equation 6 to re-calculate the Fluence rate, Φ, for each LED. The LDC correction factor obtained for each light source was applied to correct the fluence rate value, ensuring that for each wavelength the same number of photons absorbed is achieved (Table 4 and Table 5). The fluence rate for each LED prior experiments was measured using a power meter.

Table 4. Values of the initial number of photons calculated using equation 10 and the molar absorption coefficient for each wavelength.

LED	Molar Absorption Coefficient ($M^{-1}cm^{-1}$) LUZ51P (Ɛ)	Nr Initial Photons
415 nm	291817	1.67E14
505 nm	16198.7	3.00E15
630 nm	1624.9	2.99E16

Recalculating the fluence rate for each LED using the values of the Table 4 and correcting for the LDC factor, the irradiation time for each LED was defined as 40 minutes. Thus, with the value of fluence rate and with the irradiation time, the light dose value was obtained for each wavelength (Table 5).

Table 5. Values of the irradiation parameters, where Φ correspond to fluence rate; LDC correspond to Light Dose Correction; Corrected Φ correspond to the value of fluence rate corrected by the LDC factor; t, correspond to irradiation time; and LD corresponds to Light Dose.

LED	Φ (mW/cm^2)	LDC LUZ51P	LDC LUZ10P	Corrected Φ LUZ51P (mW/cm^2)	Corrected Φ LUZ10P (mW/cm^2)	t (min)	LD LUZ51P (J/cm^2)	LD LUZ10P (J/cm^2)
415 nm	0.0797	0.48	0.48	0.166	0.166		0.399	0.399
505 nm	1.18	0.56	0.61	2.11	1.93	40	5.06	4.64
630 nm	9.43	0.71	0.95	13.3	9.93		31.9	23.8

4. Results:

4.1 Molar Absorption Coefficient

The determination of the molar absorption coefficient was made preparing two stock solutions of LUZ51P, with a concentration of 0.5 mM. The two initial solutions were further diluted 10 x with DMSO to obtain a concentration of 0.05 mM. These 2 solutions were subsequently diluted in DMSO, with a final volume of 3 mL, to prepare the following concentrations: 0.83, 1.7, 3.3 and 5.0 µM. The absorption spectra of LUZ51P at the indicated concentrations were obtained using a UV-Vis spectrophotometer (Figure 11).

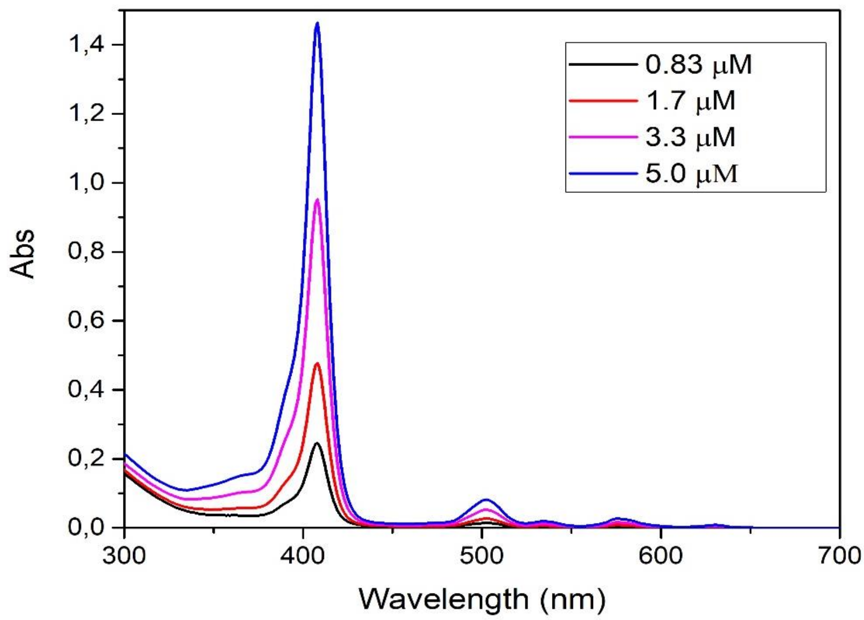

Figure 11. Absorption spectra of different concentrations, obtained from stock solution with a mass of 0.88 mg of LUZ51P.

LUZ51P is characterized by having five main absorption peaks, the highest intensity band, known as the Soret band (or B band), near 415 nm, and four other bands of lower intensity, known as Q bands. One of them, used in this work is the Soret band and the two other Q bands are located near 505 nm and at 630 nm.[50,51] The absorbance values for each maximum peaks, at 408, 502 and 630 nm, were measured using the absorption spectra corresponding to the various concentrations (Figure 11). Having the absorption values of each peak corresponding to each concentration, a linear regression of the absorbance in function of concentration (Figure 12) was performed, in which the slope corresponds to the value of the molar absorption coefficient.

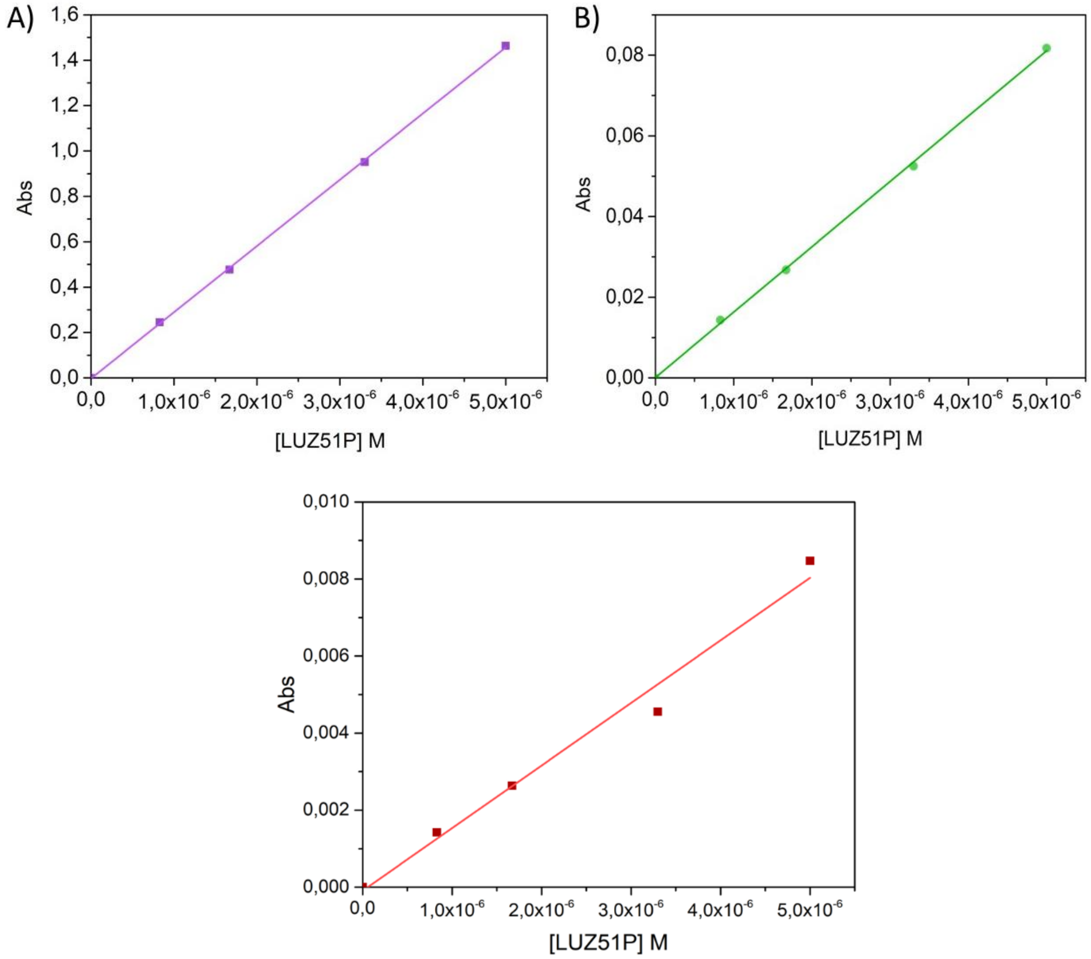

Figure 12. Absorption bands at A) 415 nm, B) 505 nm and C) 630 nm in function of concentrations of LUZ51P and the respective linear regression giving the molar absorption coefficient.

In Table 6, is presented the values of the slope giving the molar absorption coefficient to the molecule LUZ51P for each absorption band. The molar absorption coefficient for each wavelength was obtained through the average of two experiments.

Table 6. Molar absorption coefficient value for each absorption peak of LUZ51P.

Wavelength Peak (nm)	Slope Experiment 1	Slope Experiment 2	Mean	Standard Error
408	291094,67	292539,64	291817,15	722,48
502	16378,88	16018,60	16198,74	180,14
630	1636,87	1612,92	1624,90	11,97

Then, to conclude, the molar absorption coefficients of LUZ51P in DMSO are Ɛ (408 nm) = 291817 $M^{-1}cm^{-1}$, Ɛ (502 nm) = 16199 $M^{-1}cm^{-1}$ and Ɛ (630 nm) = 1625 $M^{-1}cm^{-1}$.

4.2 Singlet Oxygen Quantification

In order to quantify the number of ROS that are formed by activate LUZ51P using different wavelengths of light, a fluorescent probe was used. The probe selected was the singlet oxygen sensor green (SOG), which is relatively selective to oxygen singlet [52], which is also the unique specie produced by LUZ51P (determined by measuring the quantum yield of singlet oxygen of LUZ51P by time-resolved phosphorescence method, data not shown in this work) in the PDT process. The main purpose of using SOG, was to validate if the irradiation parameters calculated in the previous chapter were corrected. It was assumed that if the number of photons absorbed by the PS, from the three LEDs, was the same, the production of ROS must be equal for the different wavelengths. Thus, if the number of photons and the fluence rate calculations were correctly calculated, we should obtain the same fluorescence value of SOG among the three LEDs.

Then, to quantify the fluorescence of the probe, the plates containing the working solutions were irradiated with the fluence value calculated for each wavelength. After each irradiation, the SOG fluorescence was read using a microplate reader (BioTek), with $\lambda_{excitation}$ = 485/20 nm and $\lambda_{emission}$ = 530/35 nm. For the analysis of the results, a linear regression of fluorescence was performed according to the number of photons absorbed (Figure 13). In this experiment two solvents were used, methanol and RPMI, to study the effect of different solvents in generation of oxygen singlet, RPMI was used with the aim of resembling the *in vitro* conditions.

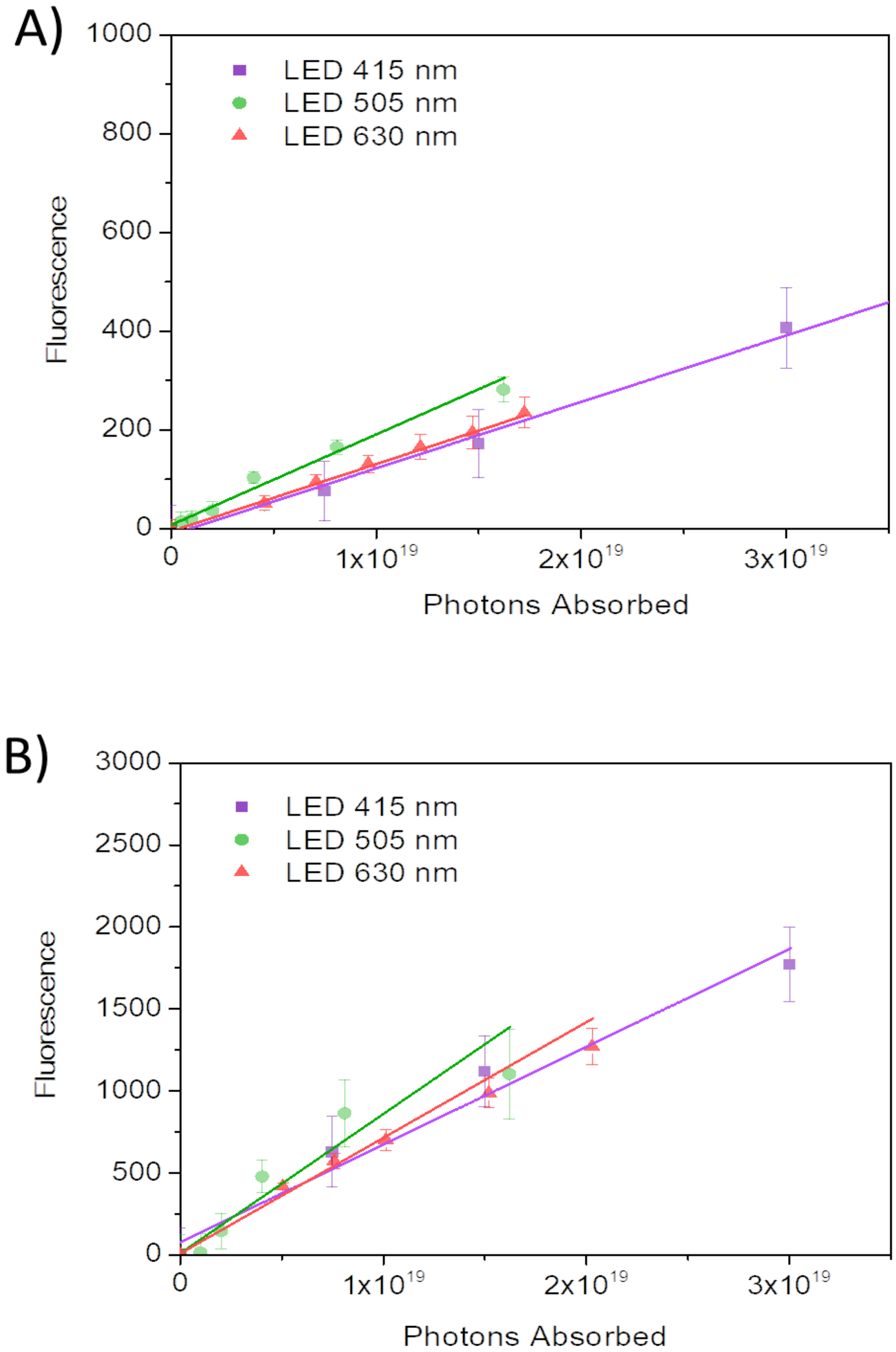

Figure 13. Fluorescence emitted by SOG in function of the number of photons absorbed, for the three wavelengths used in the irradiation. A) in methanol and B) in RPMI.

The slopes of each linear regression are relatively similar, which shows that, the fluorescence emitted by SOG does not depend on the different wavelengths, but only depend on the number of photons absorbed. The small differences that were observed in the slopes might be attributed to small experimental variations. The results confirm that the same amount of ROS was produced regardless of the LED wavelength, which in turn confirm that the irradiation conditions determined in this work permit that the same number of photons are absorbed by LUZ51P. After this validation the same conditions of irradiation were used to activate LUZ51P in *in vitro* experiments.

4.3 *In vitro* Studies

In vitro studies were conducted in 4T1 cells, a murine mammary carcinoma cell line. The purpose of using a tumor cell line was to evaluate the effect of three different wavelengths in a PDT protocol using LUZ51P or LUZ10P, which have distinct intracellular localizations. PSs that accumulate in organelles such as the ER-GA complex and/or in the mitochondria, a cell organelle involved apoptosis, are typically considered more phototoxic than PSs that accumulated in the endocytic pathway.[13]

In a first set of experiments, cytotoxicity studies were conducted with a range of concentrations for LUZ51P, varying from 12.5 to 400 nM, in order to select concentrations that are not toxic in the dark. As can be seen in Figure 14A, the concentrations of 12.5, 25.0 and 50.0 nM, show no toxicity, while higher concentrations cause toxicity in the dark. For the LUZ10P photosensitizer, a range of concentrations between 10 and 100 µM were used. From the results, shown in Figure 14B, none of the concentrations used, caused cell death in the dark.

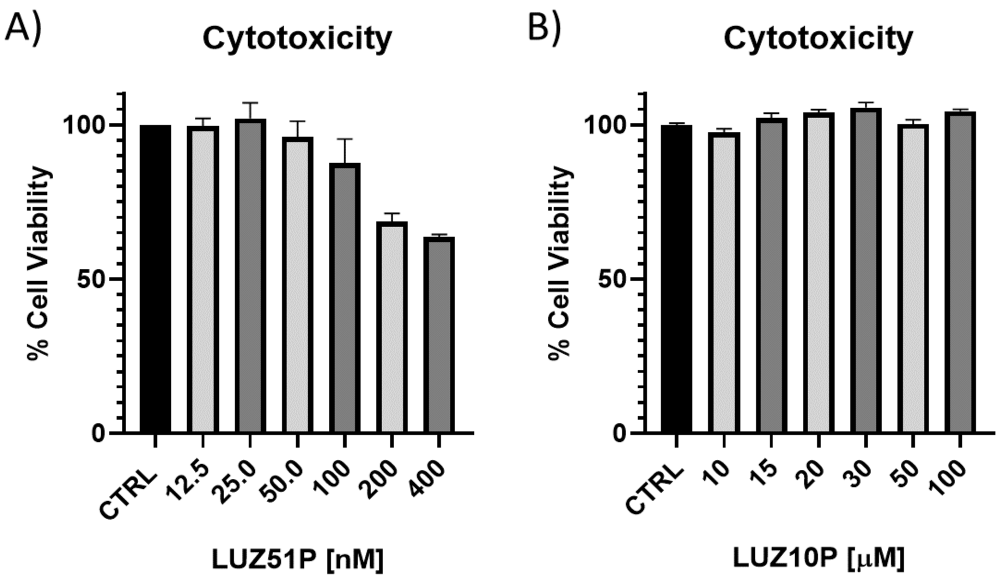

Figure 14. Evaluation of cytotoxicity in the cell line 4T1, A) of LUZ51P with concentrations varying between 12.5 and 400 nM; B) of LUZ10P with concentrations varying between 10 and 100 µM. Each bar represents the mean ± SEM of three independent experiments.

Based on the dark toxicity studies, the concentrations of 12.5, 25.0 and 50.0 nM were selected for the phototoxicity studies involving LUZ51P. Considering the lack of dark toxicity attained with LUZ10P, in the range of 10 to 100 μM, the concentrations that were used to assess biological effects were of 10 and 20 μM.

According to the Kasha's rule, it was anticipated that cell viability would be the same regardless of the wavelength utilized in PDT if the same number of photons were used. However, our results demonstrated that the different wavelengths of light induced different biological responses, resulting in different cellular viability for both PSs in this PDT protocol. Starting with the LUZ51P, where the results are shown in Figure 15, it is possible to verify that for the LEDs at 415 and at 505 nm, the decrease on the cell viability is concentration dependent. It is noticeable that, the blue light (415 nm) is the light that induce more cell death, which is followed by the green light (505 nm), and then red light (630 nm). At 630 nm, the light did not induce significant phototoxicity even for the highest concentration of LUZ51P (50 nM). In fact, for the LEDs emitting at 415 nm or 505 nm, the increase of the PS concentration to the double, causes the percentage of cell viability to decrease to a half. The LED at 630 nm, on the other hand, does not induce significative changes in cell viability with the increase of PS concentration.

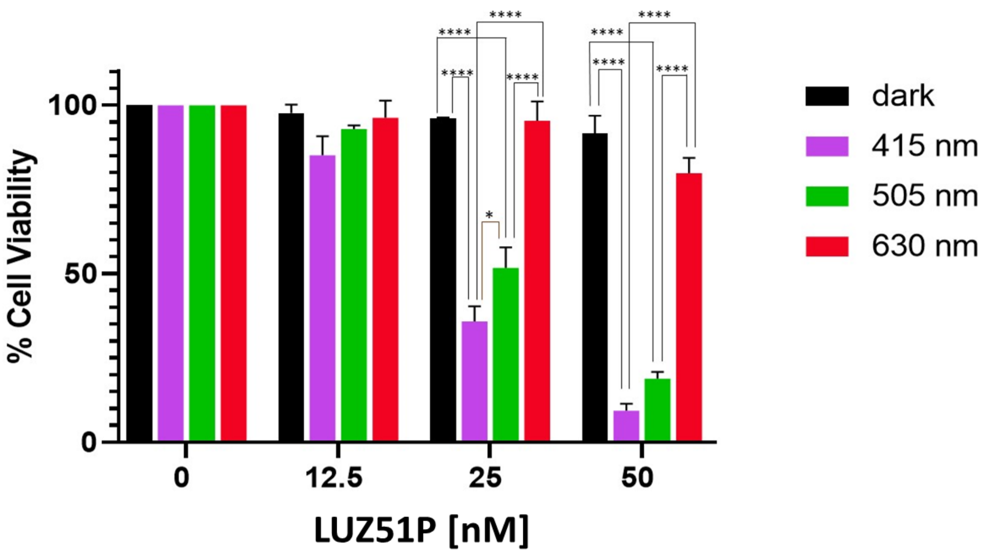

Figure 15. Phototoxicity studies using three wavelengths, 415nm, 505nm and 630nm, to activate LUZ51P in the 4T1 cell line. Each bar represents the mean ± SEM of three independent experiments. Statistical significance was evaluated using two-way ANOVA. **** $p < 0.0001$; *$p = 0.0325$.

The results obtained with LUZ10P were slightly different from those attained with LUZ51P. In LUZ10P PDT protocol, blue and green light have similar effects on decreasing cell viability which impact was higher than when red light was used. When comparing the two concentrations of LUZ10P, the effect of the three LEDs in the cell viability was inverse with the increasing of concentrations, meaning that, when the concentration doubles, the cell viability for the three wavelengths decrease by a half (Figure 16).

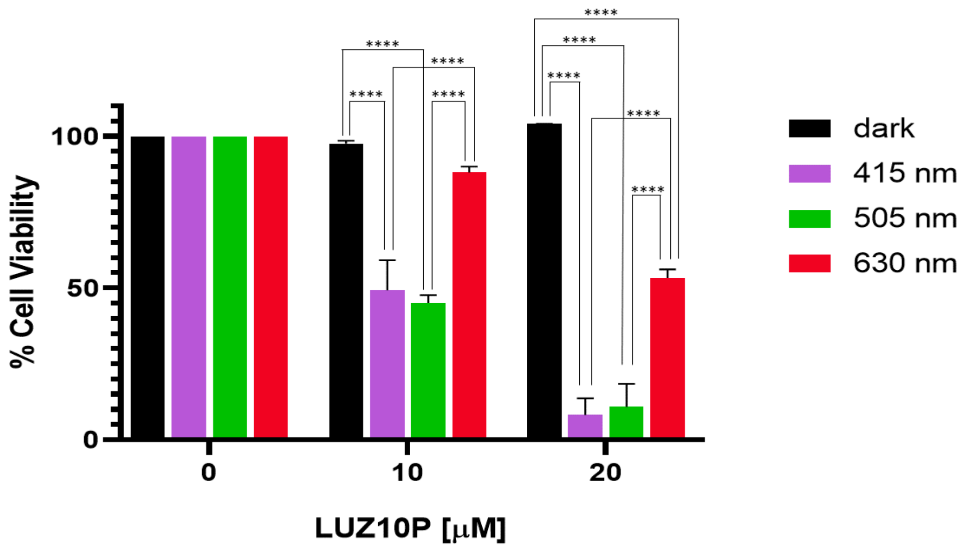

Figure 16. Phototoxicity studies using three wavelengths, 415 nm, 505 nm and 630 nm, to activate LUZ10P in the 4T1 cell line. Each bar represents the mean ± SEM of three independent experiments. Statistical significance was evaluated using two-way ANOVA. **** $p < 0.0001$.

Analysing the Figure 15 with the results obtained with the LUZ51P molecule, it can be seen that with the lowest concentration, 12.5 nM, blue light resulted in a cell viability of 85%, green light in 93% and red light in 95%. For 25 nM, the cell viability decreased to 36% using blue light, to 52% with green light and with red light the cell viability remained at 95%. Finally, for the highest concentration, 50 nM, cell viability decreased to 9% when blue light was applied, 19% with green light and 80% with red light. These results demonstrated that with increasing concentration, cell viability for blue and green light decreases approximately by half, while the use of red light for the concentration of 50 nM causes a decrease of approximately 15%. For LUZ10P, Figure 16, using 10 µM, cell viability percentages of 49% and 45% were obtained when blue and green LEDs were applied, respectively. While the red LED resulted in a cell viability of 88%. At the concentration of 20 µM, cell viability was 8% for blue light, 11% for green light and 53% for red light. Overall, the decrease in cell viability induced by LUZ10P activated by blue and green light is identical. This contrast with the results obtained with LUZ51P where the highest impact was found for blue light. In addition, for LUZ51P, the LED at 630 nm had almost no effect on the cell viability, while with LUZ10P there was a significant effect of red light, which reduced cell viability as the LUZ10P concentrations increased.

Overall, these results suggest that the intracellular localization of the PSs significantly influences their phototoxicity as well as the outcomes of PDT when using different wavelengths. These findings may indicate the presence of distinct synergistic effects, not only due to the variations in wavelengths but also as a result of different intracellular localizations. Considering that cytochrome c has an endogenous porphyrin chromophore with an absorption spectrum showing a Soret band at 408 nm and weaker bands at approximately 530 nm, it was hypothesized that the differences observed in the PDT effect at the different wavelengths may be related with the absorption of light by the cytochrome c. Interestingly, when comparing the effects of blue and green light on cell viability using LUZ10P, the results were virtually similar. This observation raises the possibility that the involvement of cytochrome c in cell viability may be less pronounced when using LUZ10P compared to LUZ51P. One plausible explanation for this could be that LUZ10P does not preferentially accumulate in the mitochondria, leading to less stimulation of cytochrome c in these organelles. Consequently, the reduced mitochondrial involvement might account for the minimal difference observed between the two wavelengths (415 and 505 nm) which contrasts with LUZ51P. The involvement of cytochrome c in the varied phototoxicity of LUZ51P upon activation at different wavelengths may indicate that apoptosis is potentially implicated in the phototoxicity of LUZ51P. So, next mechanism of cell death of LUZ51P-PDT was investigated.

4.4 Fluorescence Microscopy

A follow up study to confirm the type of cell death triggered by PDT using LUZ51P, was performed by fluorescence microscopy. Cells were incubated with different concentrations of LUZ51P (12.5, 25 and 50 nM) and 3 hours after the irradiation, using the same irradiation conditions as mentioned on the previous studies, Hoechst 3342 and Propidium iodide (PI) were added to the cells for 20 minutes.

Hoechst are a family of blue-fluorescent dyes, used as a nuclear DNA marker dye. In particular, Hoechst 33342 is used to distinguish apoptotic cells from live cells. It allows to identify cells in the process of apoptosis through the detection of condensation and fragmentation of chromatin, which are hallmarks of apoptosis.[53] PI is a red fluorescence dye that only marks dead cells because it only permeates cells with the plasma membrane compromised, where it complexes with DNA. The simultaneous use of these two dies makes it possible to distinguish health, apoptotic and dead cells, through cell morphology.

A

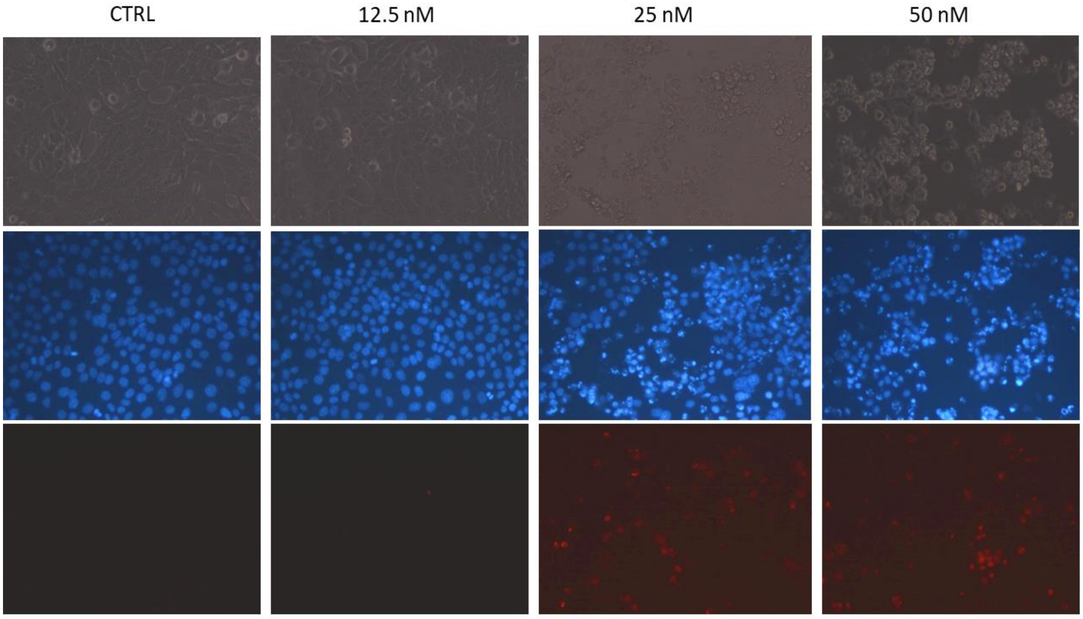

B

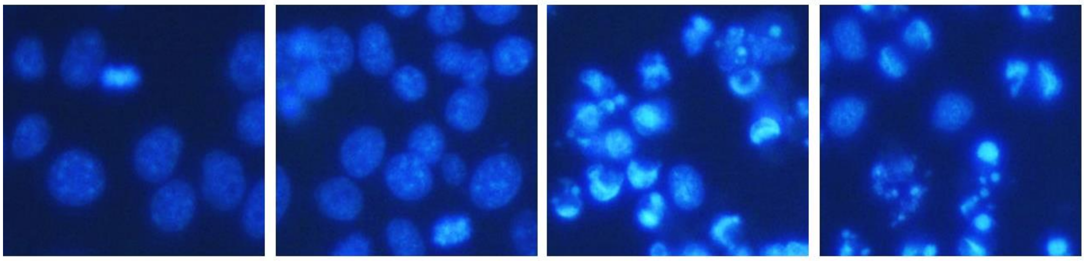

Figure 17. A) Representative images of fluorescence microscopy, with cells irradiated with blue light (415 nm), in the absence of PS (CTRL) and with the presence of PS at different concentrations (12.5, 25.0 e 50.0 nM). The first row of images corresponds to the morphology of the cells, without the use of a fluorescent dye; the second row corresponds to nucleus stained with Hoechst (blue); and in the last row, corresponds to dead cells stained with propidium iodide (red). B) Cropped section from the original images in (A), zoomed in to highlight the differences in the nucleus morphology in response to PS concentration.

Figure 17 corresponds to images depicting cell morphology and Hoechst and PI staining, when 4T1 cells were irradiated with blue light (415 nm). In the control group, without PS, it is possible to observe, by the morphology of cells, that exists a homogenous distribution of Hoechst dye on the cell nuclei. As expected, no PI signal was observed, which indicates the absence of dead cells. In contrast, with the introduction of LUZ51P it is noticeable that with increasing concentrations of PS, there is an increase on the fluorescence signal from PI dye, meaning the increase in the number of dead cells. With the Hoechst marker it is possible to verify that with the increase of the concentration of PS, there is more apoptotic cells, because there are more cells with condensed and fragmented chromatin, characteristics of cells in the process of apoptosis. The aim of this first experiment was to verify whether cell death caused by light, in this case blue light, was a regulated form of cell death, such as apoptosis. The fact that we have observed signs of apoptotic cells allows us to anticipate the involvement of cytochrome c in the mode of action of LUZ51P. This hypothesis is based in the fundamental role of cytochrome c in the apoptotic process as well as aby the presence of a porphyrin group in its structure.

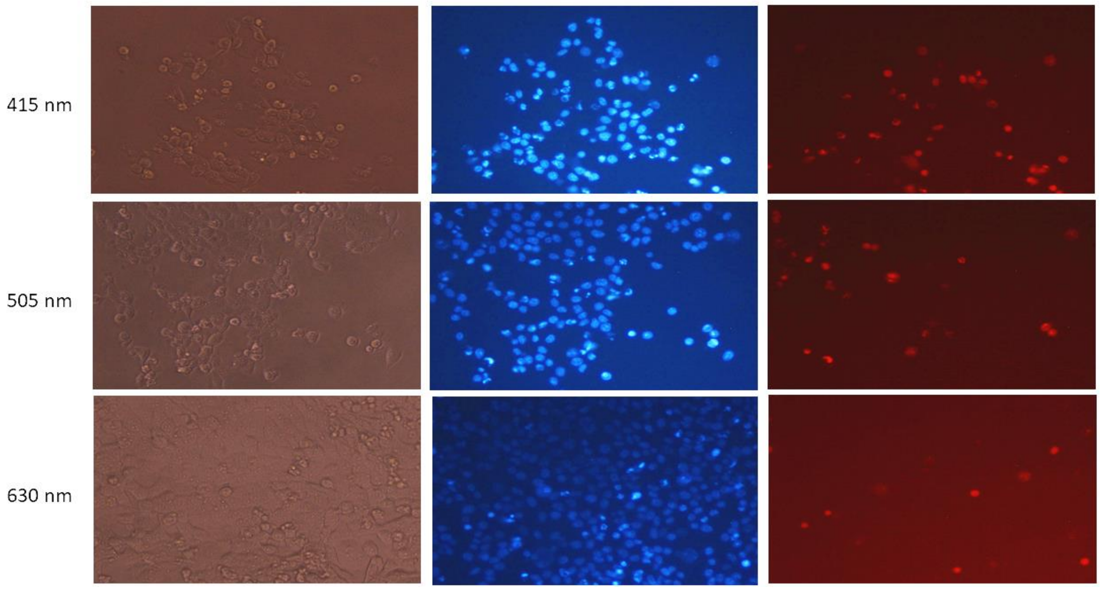

Figure 18. Representative images of fluorescence microscopy, with cells irradiated with blue light (415 nm), green light (505 nm) and red light (630 nm) in the presence of 100 nM of concentration of LUZ51P. The first column of images corresponds to the morphology of the cells, without the use of a fluorescent dye; the second column corresponds to nucleus stained with Hoechst (blue); and in the last column, corresponds to dead cells stained with propidium iodide (red).

In PDT, if the number of photons absorbed is the same regardless of wavelength, the expected result is that cell viability would be the same across all conditions, and the type of cell death would also be the same. So, the second study using fluorescence microscopy was aimed at evaluating differences in cell viability and/or type of cell death produced by the different wavelengths, 415 nm (blue), 505 nm (green) and 630 nm (red). The results in the Figure 18 show that with blue light, at 415 nm, there is more cell death and mostly caused by apoptosis This is possible to observe by the higher PI fluorescence in the treated cells, indicating the presence of more dead cells, and there was a gradual decrease in fluorescence to the green light, at 505 nm and then to the red light, at 630 nm, where there is considerably less cell death. The Hoechst dye permit to confirm that most of dead cells present changes in chromatin, such as condensation or fragmentation, which are hallmarks of the regulated cell death process, namely apoptosis. This type of cell death is predominant in the three wavelengths used, indicating that there are different amounts of cell viability among wavelengths, but the type of cell death is the same. Thus, these results suggest that other biological effects, beyond the effect caused by PDT through the formation of ROS, might be elicited by blue and/or green lights.

Considering the indices of apoptosis, it was hypothesized that the source of the synergistic effects observed at 415 nm light involve cytochrome c. The release of this protein from the mitochondria into the cell cytosol is an important step in the apoptosis process. This release can occur through pores on the mitochondrial membrane that are formed by two proteins, BAX and BAK. In the cytosol, cytochrome c is involved in the formation of the apoptosome and consequent activation of caspases that results in apoptosis. In addition to this important function, cytochrome c has a porphyrin as its chromophore, which has an absorption spectrum (Figure 19) characterized by a strong absorption peak at 400 nm and at 505 nm. Therefore, having a Soret band at approximately 415 nm, blue light induces the oxidation of cytochrome c, i.e., it changes redox form from the Fe^{2+} state to the Fe^{3+} state, and only the oxidized state allows the formation of the apoptosome and consequent induction of apoptosis.[54,55] Thus, it is suggested that irradiation with blue light, may cause an increase in apoptosis, which justifies the differences observed when evaluating the cell viability at the chosen three wavelengths. Hence, in order to study the influence that cytochrome c has on the results of cell viability, a BAX protein inhibitor, which prevents the release of cytochrome c from the mitochondria to the cytosol, was tested.

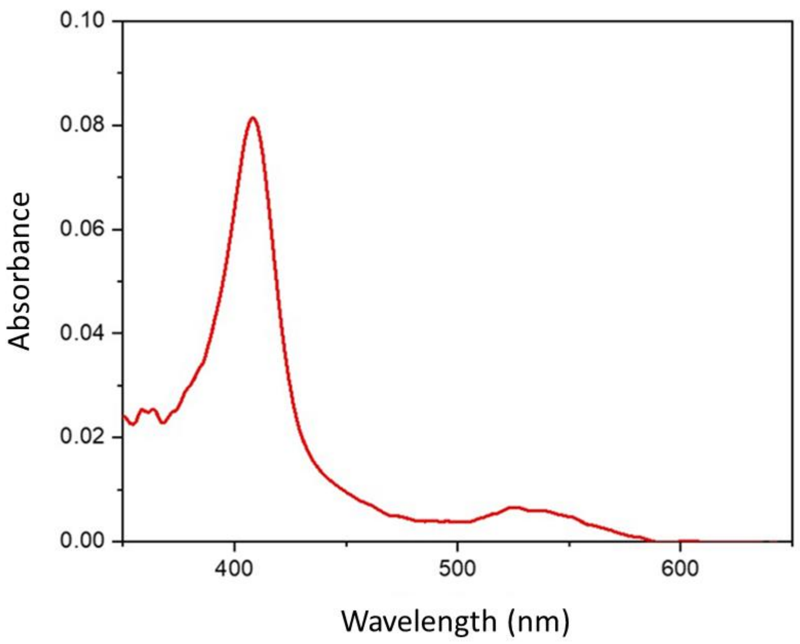

Figure 19. Absorption spectrum of cytochrome c in PBS (obtained on this work).

4.5 Impact of the cytochrome c inhibitor BAI-1 on cell viability

BAI-1 (1-(3,6-dibromo-carbazol-9-yl)-3-piperazin-1-yl-propan-2-ol) is a molecule that specifically inhibits the Bax protein's channel-forming activity.[56] BAX is a pro-apoptotic protein belonging to the BCL-2 family, which plays a critical role in regulating apoptosis. During apoptosis, BAX undergoes conformational changes, leading to the formation of channels in the mitochondrial outer membrane, allowing the release of cytochrome c from the mitochondria into the cytosol. By blocking the channel-forming activity of BAX, BAI-1 aims to prevent the release of cytochrome c and inhibit the apoptotic pathway. Thus, the use of BAI-1 may potentially protect cells from undergoing apoptosis, and this effect is expected to be more pronounced when combined with light at 415 nm or 505 nm, ultimately promoting cell survival.[57]

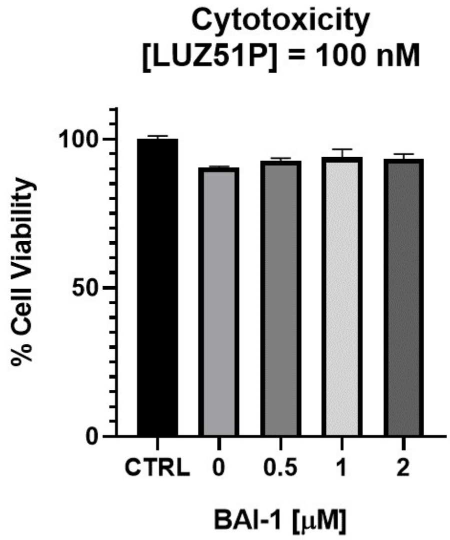

Figure 20. Cytotoxicity studies, using BAI-1 and 100 nM of LUZ51P, on the 4T1 cell line. Each bar represents the mean ± SEM of one independent experiment.

According to the results obtained from cytotoxicity studies (Figure 20), the applied concentrations of BAI-1 did not demonstrate toxicity in the dark when combined with LUZ51P.

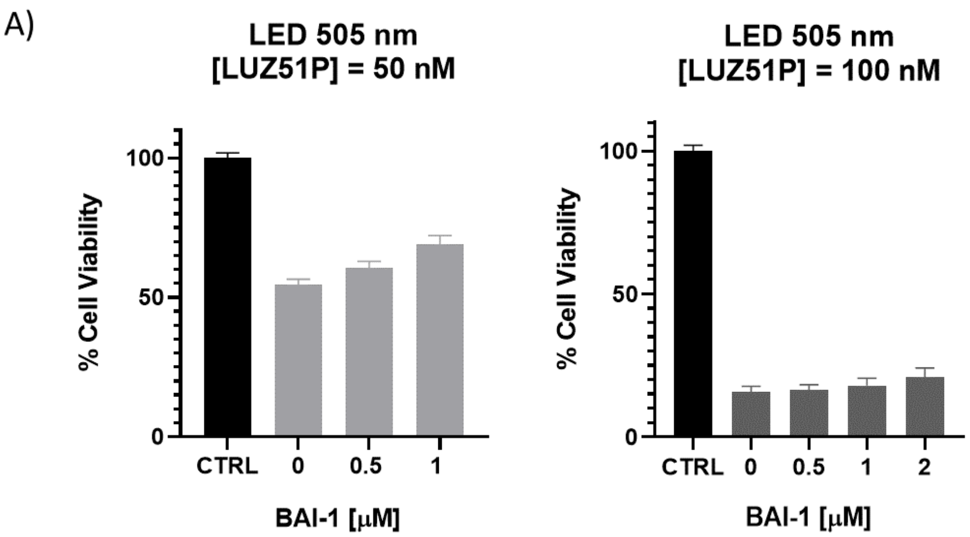

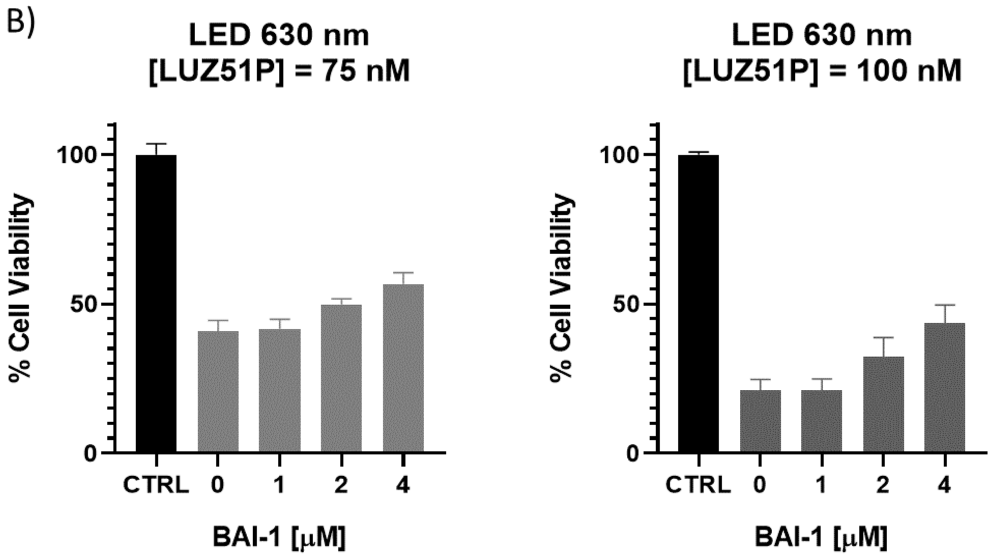

Figure 21. Phototoxicity studies, using BAI-1, on the 4T1 cell line. A) Phototoxicity assay using 50 nM and 100 nM of LUZ51P, using the LED at 505 nm; and B) Phototoxicity assay using 75 nM and 100 nM of LUZ51P, using the LED at 630 nm. Each bar represents the mean ± SEM of one independent experiment.

Preliminary studies were conducted applying the BAX protein inhibitor, BAI-1, in combination with LUZ51P to investigate cell viability behaviour under different wavelengths. Green light at 505 nm and red light at 630 nm were used for this experiment. Initially, based on the results obtained from activating the PS with different wavelengths, a hypothesis was proposed, suggesting that cytochrome c played a crucial role in PDT, being involved in a synergistic process. This synergistic process resulted in reduced cell viability when the PS was activated with blue and green light compared to red light. This hypothesis was supported when the same protocol was applied using a hydrophilic photosensitizer, LUZ10P, which led to decreased cell viability when activated with blue and green light.

However, the results from these preliminary studies, which require further confirmation, showed an unexpected increase in cell viability when BAI-1 was added to the PDT protocol, not only with green light but also with red light. As shown in Figure 21A, for the 505 nm LED, were used concentrations of 50 nM and 100 nM of LUZ51P. At the 50 nM concentration, the inhibitor had a more pronounced effect compared to the results obtained with the higher concentration. While the 50 nM concentration resulted in 54% cell viability, the addition of 1 µM BAI-1 increased cell viability to 69%, indicating a protection effect from the inhibitor. However, with the 100 nM concentration of LUZ51P, which resulted in 16% cell viability, the addition of the same concentration of BAI-1 only increased cell viability to 18%. These results can be explained by the diminished capacity of the inhibitor to reverse the process of cell death when cell viability is already low. With red light, higher concentrations of LUZ51P were required to induce cell death, using concentrations of 75 nM and 100 nM. With red light, the effect of the BAI-1 inhibitor was observed for both concentrations of LUZ51P, which was not the case with green light. At a 75 nM LUZ51P concentration, it caused 41% cell viability, but when the BAI-1 inhibitor at 2 µM and 4 µM was introduced, cell viability increased to 50% and 57%, respectively. These results indicate an enhancement of cell viability and, consequently, an inhibition of apoptotic cell death. The same effect was observed with 100 nM LUZ51P, where the PS alone resulted in 21% cell viability, but the presence of 2 µM and 4 µM BAI-1 inhibitor increased cell viability to 32% and 44%, respectively.

Based on our hypothesis, we would expect higher protection from BAI-1 when green light was used, as opposed to the red light. However, our results showed similar levels of protections for both wavelengths. This suggests that cytochrome c is involved in cell death mediated by LUZ51P regardless of the light wavelength. While not disregarding these results, as they are equally interesting and valuable for future studies, further research is needed to explain the synergistic mechanisms involved when blue and green light were used. Of note, the latter increase approximately 50% the cell death, an effect that cannot solely be attributed to PDT-mediated ROS. The ongoing investigations aim to clarify the underlying mechanisms responsible for the observed synergistic effects and elucidate the specific factors contributing to the complexity of this process.

5. Discussion

According to Kasha's rule, the number of photons absorbed is crucial in PDT, rather than the energy of photons. When molecules are excited to an upper excited state (Sn), they subsequently return to the S1 excited state before entering the triplet excited state (T1), where they transfer energy to molecular oxygen, generating ROS. Following this rule, a PDT protocol with different wavelengths but the same number of photons absorbed by the PS, should produce the same biological effect. To test this premise, our study examined three wavelengths (415 nm, 505 nm and 630 nm) and two PSs with different sub-cellular localizations. LUZ51P, a hydrophobic compound (LogP ca. 3), accumulates in cellular organelles such as the ER, Golgi apparatus and mitochondria, possibly enhancing its phototoxic capacity. In contrast, LUZ10P is a soluble molecule (LogP = -1.4), accumulating in lysosomes with lower phototoxic capacity.

The results obtained contradict the expected effect predicted by Kasha's rule. When using LUZ51P, blue light induces the lowest cell viability, approximately 36%, followed by green light about 52%, and red light showed almost no cell death, resulting in 95% of cell viability. With LUZ10P, blue and green light had almost identical effects, with cell viabilities of 8% and 10%, respectively. However, red light caused cell death, resulting in 53% cell viability. Li et al had shown, even without having the same number of photons absorbed, that blue light caused a higher photodynamic effect compared to red light. In this work, accounting for the correctly same number of photons absorbed, similar results were obtained.[5] The discrepancy between the three wavelengths highlights that PDT biological outcomes do not depend only on the ROS produced, but also in the wavelength used (Figure 22) and the PS intracellular localization. The wavelength impact on the cellular viability is the most astonishing result of our work. These observations suggest that using blue light, instead of red light, may be beneficial (even though with less light penetration across the tissues), as synergies with endogenous compounds can be triggered, including effect on the immune system. Based on this work, a novel approach is proposed involving a device that integrates simultaneously distinct LEDs emitting at 415, 505, and 630 nm (Figure 23). The blue and green light contribute to an enhancement of photodynamic effect on the surface of tissues, while the red light facilitates deeper tissue penetration.

Considering that the different wavelengths resulted in distinct amounts of cell viabilities, the type of cell death associated with LUZ51P was studied. Due to its chemical characteristics, LUZ51P tends to be easily internalized by cells and accumulates in ER-GA, which may imply more cell death, due to the fact that damage in these organelles act upstream to the intrinsic pathway of apoptosis.[58] This study revealed that the predominant type of cell death was apoptosis, with a higher percentage of death by apoptosis observed with blue light, followed by green light and red light, having the least effect. In apoptosis, a critical protein is the cytochrome c, which contains a porphyrin in its chemical structure, with absorption bands approximately at 415 and 505 nm, corresponding to the absorption peaks of the PSs that were used. This suggests that the effects observed with blue and green light may be justified through a synergistic process involving PDT and cytochrome c.

To understand the importance of cytochrome c in the observed cell viability responses, it was used an inhibitor of the BAX protein, responsible for releasing of cytochrome c from mitochondria to the cytosol. By blocking the BAX protein, it was expected that the release of cytochrome c would not occur, and consequently, cell death by apoptosis would not take place. This was in fact observed for both the green and red light, which confirms apoptosis as the main mechanism of cell death regardless the light wavelength. However, this result does not permit to confirm cytochrome c as the main player of the synergistic effects observed with the blue and green light.

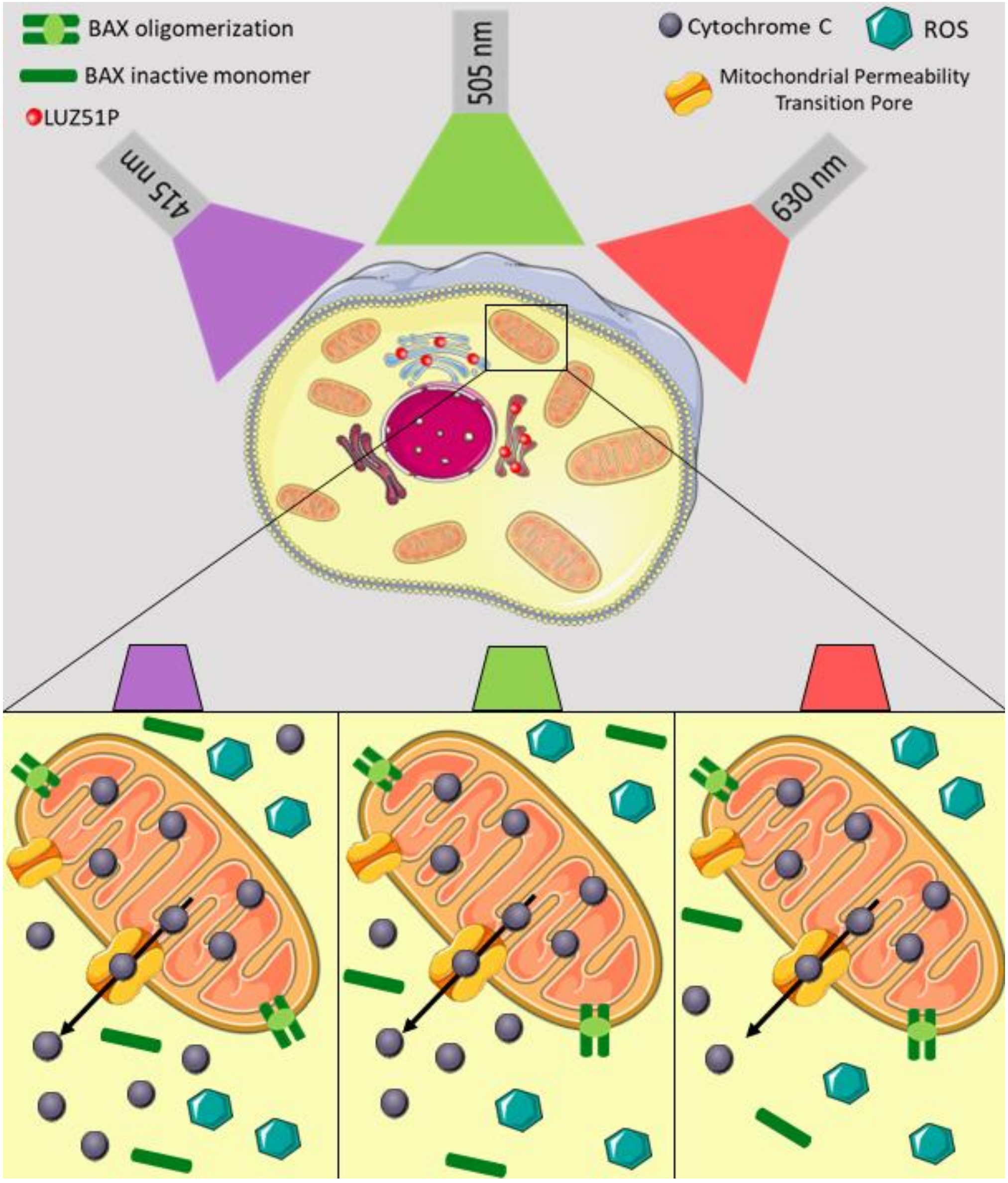

Figure 22. Schematic representation of the proposed mechanism activation of the PS LUZ51P with the three wavelengths, 415, 505 and 630 nm produces the same amount of ROS but enhanced cytochrome c release is only attained at 415 and 505 wavelength.

6. Conclusion

The main goal of this master thesis was to analyze the impact of different wavelengths, 415, 505 and 630 nm, on the phototoxicity of a PDT protocol. The main conclusion drawn from the obtained results was that when the same number of photons was absorbed using different wavelengths, each type of light affected cell viability differently. According to Kasha's rule, the effect of light in PDT should be independent of the wavelength for the same number of photons absorbed. When different wavelengths produce the same number of photons absorbed, it would be expected that the same biological responses are attained. To confirm this premise, calculations were made to equalize the number of photons absorbed for the three LEDs with the following maximum wavelengths: 415, 505, and 630 nm. From the number of photons absorbed, the fluence rate values for each LED were calculated and the irradiation time was set at 40 minutes. Two PSs, LUZ51P and LUZ10P, with different intracellular localizations, were selected to study the effect of light on the PDT effect. As such, in a first approach, cytotoxicity and phototoxicity studies were conducted on the 4T1 cell line. At this stage, it was possible to realize that light, in its different ranges, produced different biological effects, and there were also distinct effects between PSs. For LUZ51P there was a distinct response for each LED. The highest phototoxicity for LUZ51P was observed for the LED at 415 nm followed by the LED at 505 nm, with a difference of approximately 10% in cell viability between these two LEDs. Interestingly, no decrease on the cell viability was observed when LUZ51P was activated with light at 630 nm, while the blue light caused approximately 60% more cell death compared to the red light. The activation of LUZ10P with the three wavelengths resulted in similar cell viabilities when using blue (415 nm) and green (505 nm) light. However, the cell viability was approximately 40% lower when activated with red light (630 nm). Comparing the two photosensitizers (PSs), it becomes evident that LUZ51P exhibits higher cell death with blue light compared to the other two wavelengths, whereas for LUZ10P, the cell viability results are similar for blue and green light. Interestingly, when activated with the 630 nm LED, LUZ51P does not induce cell death, while LUZ10P does lead to cell death. It was shown that regulated cell death, namely apoptosis, is the mechanism of cell death that is operating after photoactivation of LUZ51P. Interestingly, the percentage of apoptosis differs when comparing the different wavelengths, with blue light inducing more apoptosis compared to green and red light. For apoptosis to occur, the cytochrome c (whose chromophore is a porphyrin) is a fundamental element. With this evidence, the hypothesis of a synergistic effect between the endogenous compound, cytochrome c, and light at 415 and 505 nm was suggested, justifying the different cellular responses. The inhibition of the BAX protein through the use of an inhibitor, BAI-1, and activation of the LUZ51P molecule with green light (505 nm) and red light (630 nm) revealed an increase in cell viability when applying red light, regardless of the PS concentration. However, with the use of green light, it was observed that at the lower PS concentration, the presence of the inhibitor caused a slight increase in cell viability, but at the higher PS concentration, there was no effect of BAI-1. These preliminary results suggest that there is a more complex biological mechanism beyond the involvement of cytochrome c, as initially hypothesized, which may explain the observed synergistic effect when applying blue and green light. However, these experiments should be extended to the other wavelength at 415 nm, and also explore the use of other inhibitors targeting other biochemical pathways. This approach should help elucidate the different outcomes obtained for cell viability when using different wavelengths, allowing a deeper understanding of the underlying mechanisms involved. By exploring other inhibitors, we can potentially identify specific molecular targets responsible for the synergistic process in cell viability, providing valuable insights into the complex interplay of biological processes and light wavelength in the context of photodynamic therapy.

The innovative device (Figure 23) and protocol resulted of this work holds promise in the realm of PDT treatment. By harnessing the unique attributes of each wavelength, it is possible to optimize the PDT outcomes. The combination of these three wavelengths and the synergistic effects of blue and green light plus the deep optical depth of red light has the potential to revolutionize PDT therapies, including possible stimulation of the immune system.

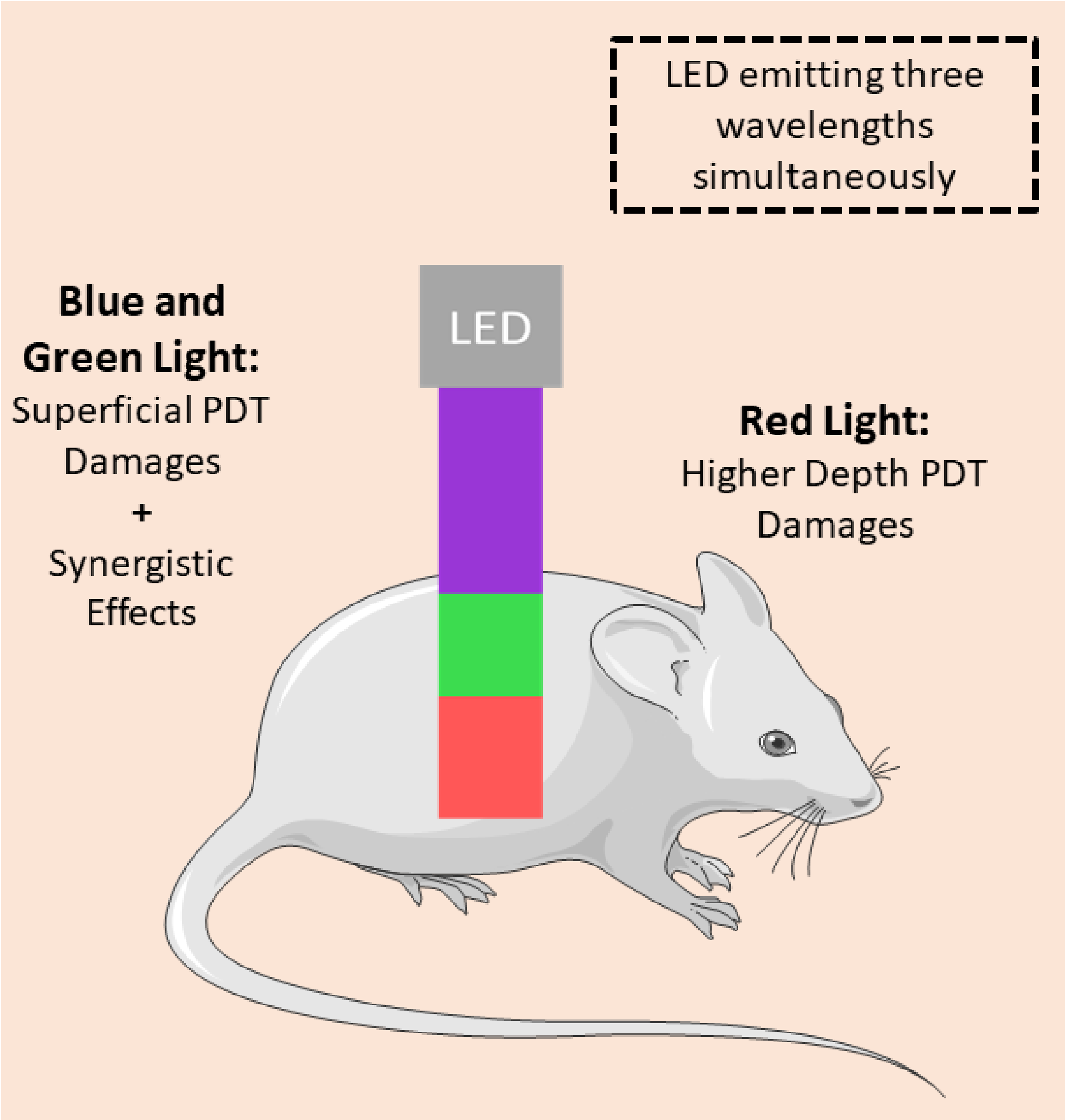

Figure 23. Proposed PDT device based on the master dissertation conclusion.

References

1. Serrage, H. *et al.* Under the spotlight: Mechanisms of photobiomodulation concentrating on blue and green light. *Photochem. Photobiol. Sci.* **18**, 1877–1909 (2019).
2. Negri, L. B., Martins, T. J., da Silva, R. S. & Hamblin, M. R. Photobiomodulation combined with photodynamic therapy using ruthenium phthalocyanine complexes in A375 melanoma cells: Effects of nitric oxide generation and ATP production. *J. Photochem. Photobiol. B Biol.* **198**, 111564 (2019).
3. Kwiatkowski, S. *et al.* Photodynamic therapy – mechanisms, photosensitizers and combinations. *Biomed. Pharmacother.* **106**, 1098–1107 (2018).
4. Cios, A. *et al.* Effect of different wavelengths of laser irradiation on the skin cells. *Int. J. Mol. Sci.* **22**, 1–19 (2021).
5. Li, X. *et al.* A novel 450-nm laser-mediated sinoporphyrin sodium-based photodynamic therapy induces autophagic cell death in gastric cancer through regulation of the ROS/PI3K/Akt/mTOR signaling pathway. *BMC Med.* **20**, 1–20 (2022).
6. Opländer, C. *et al.* Effects of blue light irradiation on human dermal fibroblasts. *J. Photochem. Photobiol. B Biol.* **103**, 118–125 (2011).
7. Del Valle, J. C. & Catalán, J. Kasha’s rule: A reappraisal. *Phys. Chem. Chem. Phys.* **21**, 10061–10069 (2019).
8. M. Kasha, Discuss. Faraday Soc., 1950, 9, 14–19.
9. Schaberle, F. A. Assessment of the actual light dose in photodynamic therapy. *Photodiagnosis Photodyn. Ther.* **23**, 75–77 (2018).
10. Luz, A. F. S., Pucelik, B., Pereira, M. M., Dąbrowski, J. M. & Arnaut, L. G. Translating phototherapeutic indices from in vitro to in vivo photodynamic therapy with bacteriochlorins. *Lasers Surg. Med.* **50**, 451–459 (2018).
11. Dąbrowski, J. M. & Arnaut, L. G. Photodynamic therapy (PDT) of cancer: from local to systemic treatment †. *Photochem. Photobiol. Sci.* **14**, 1765 (2015).
12. Donohoe, C., Senge, M. O., Arnaut, L. G. & Gomes-da-Silva, L. C. Cell death in photodynamic therapy: From oxidative stress to anti-tumor immunity. *Biochim. Biophys. Acta - Rev. Cancer* **1872**, 188308 (2019).
13. Moserova, I. & Kralova, J. Role of er stress response in photodynamic therapy: Ros generated in different subcellular compartments trigger diverse cell death pathways. *PLoS One* **7**, (2012).
14. Kessel, D. Subcellular Targeting as a Determinant of the Efficacy of Photodynamic Therapy. *Photochem. Photobiol.* **93**, 609–612 (2017).

15. Chen, C. *et al.* Photodynamic-based combinatorial cancer therapy strategies: Tuning the properties of nanoplatform according to oncotherapy needs. *Coord. Chem. Rev.* **461**, 214495 (2022).
16. Abrahamse, H. & Hamblin, M. R. New photossensitizersfot photodynamic therapy. *Biochem. J.* **473**, 347–364 (2017).
17. Lobo, C. S., Gomes-da-Silva, L. C. & Arnaut, L. G. Potentiation of Systemic Anti-Tumor Immunity with Photodynamic Therapy Using Porphyrin Derivatives. in 279–344 (2022). doi:10.1142/9789811246760_0222.
18. Arnaut, L. G. *et al.* Photodynamic Therapy Efficacy Enhanced by Dynamics: The Role of Charge Transfer and Photostability in the Selection of Photosensitizers. *Chem. - A Eur. J.* **20**, 5346–5357 (2014).
19. Li, X. *et al.* Phthalocyanines as medicinal photosensitizers: Developments in the last five years. *Coord. Chem. Rev.* **379**, 147–160 (2019).
20. Baskaran, R., Lee, J. & Yang, S. Clinical development of photodynamic agents and therapeutic applications. *Biomater. Res.* **22**, 25 (2018).
21. Plaetzer, K., Krammer, B., Berlanda, J., Berr, F. & Kiesslich, T. Photophysics and photochemistry of photodynamic therapy: fundamental aspects. *Lasers Med. Sci.* **24**, 259–268 (2009).
22. Aroso, R. T., Schaberle, F. A., Arnaut, L. G. & Pereira, M. M. Photodynamic disinfection and its role in controlling infectious diseases. *Photochem. Photobiol. Sci.* **20**, 1497–1545 (2021).
23. Dougherty, T. J. *et al.* Photodynamic therapy. *J. Natl. Cancer Inst.* **90**, 889–905 (1998).
24. Zhang, J. *et al.* An updated overview on the development of new photosensitizers for anticancer photodynamic therapy. *Acta Pharm. Sin. B* **8**, 137–146 (2018).
25. Mussini, A. *et al.* Targeted photoimmunotherapy for cancer. *Biomol. Concepts* **13**, 126–147 (2022).
26. Chan, W. M., Lim, T. H., Pece, A., Silva, R. & Yoshimura, N. Verteporfin PDT for non-standard indications-a review of current literature. *Graefe's Arch. Clin. Exp. Ophthalmol.* **248**, 613–626 (2010).
27. Takakura, H. *et al.* Analysis of the triplet-state kinetics of a photosensitizer for photoimmunotherapy by fluorescence correlation spectroscopy. *J. Photochem. Photobiol. A Chem.* **408**, 1–6 (2021).
28. Osaki, T. *et al.* Efficacy of 5-aminolevulinic acid in photodynamic detection and photodynamic therapy in veterinary medicine. *Cancers (Basel).* **11**, (2019).
29. Penetra, M., Arnaut, L. G. & Gomes-da-silva, L. C. Trial watch : an update of clinical advances in photodynamic therapy and its immunoadjuvant properties for cancer treatment. *Oncoimmunology* **12**, 1–20 (2023).

30. Kroemer, G. *et al.* Classification of Cell Death 2009. *Cell Death Differ.* **16**, 3–11 (2009).
31. Mroz, P., Yaroslavsky, A., Kharkwal, G. B. & Hamblin, M. R. Cell death pathways in photodynamic therapy of cancer. *Cancers (Basel).* **3**, 2516–2539 (2011).
32. Piette, J. Signalling pathway activation by photodynamic therapy: NF-κB at the crossroad between oncology and immunology. *Photochem. Photobiol. Sci.* **14**, 1510–1517 (2015).
33. D'Arcy, M. S. Cell death: a review of the major forms of apoptosis, necrosis and autophagy. *Cell Biol. Int.* **43**, 582–592 (2019).
34. Strasser, A., Connor, L. O. & Dixit, V. M. Poptosis ignaling. *Annu. Rev. Biochem.* **69**, 217–45 (2000).
35. Sinha, K., Das, J., Pal, P. B. & Sil, P. C. Oxidative stress: The mitochondria-dependent and mitochondria-independent pathways of apoptosis. *Arch. Toxicol.* **87**, 1157–1180 (2013).
36. Aniogo, E. C., George, B. P. A. & Abrahamse, H. Role of Bcl-2 Family Proteins in Photodynamic Therapy Mediated Cell Survival and Regulation. *Molecules* **25**, (2020).
37. Garner, T. P. *et al.* Small-molecule allosteric inhibitors of BAX. *Nat. Chem. Biol.* **15**, 322–330 (2019).
38. Ow, Y. L. P., Green, D. R., Hao, Z. & Mak, T. W. Cytochrome c: Functions beyond respiration. *Nat. Rev. Mol. Cell Biol.* **9**, 532–542 (2008).
39. Sinibaldi, F. *et al.* Extended cardiolipin anchorage to cytochrome c: A model for protein-mitochondrial membrane binding. *J. Biol. Inorg. Chem.* **15**, 689–700 (2010).
40. Capdevila, D. A. *et al.* Active Site Structure and Peroxidase Activity of Oxidatively Modified Cytochrome c Species in Complexes with Cardiolipin. *Biochemistry* **54**, 7491–7504 (2015).
41. Su, Z., Yang, Z., Xu, Y., Chen, Y. & Yu, Q. Apoptosis, autophagy, necroptosis, and cancer metastasis. *Mol. Cancer* **14**, 1–14 (2015).
42. de Assis, L. V. M., Tonolli, P. N., Moraes, M. N., Baptista, M. S. & de Lauro Castrucci, A. M. How does the skin sense sun light? An integrative view of light sensing molecules. *J. Photochem. Photobiol. C Photochem. Rev.* **47**, 100403 (2021).
43. Bonnans, M. *et al.* Blue light: Friend or foe ? *J. Photochem. Photobiol. B Biol.* **212**, 0–7 (2020).
44. Young, A. R. Chromophores in human skin. *Phys. Med. Biol.* **42**, 789–802 (1997).
45. Wondrak, G. T., Jacobson, M. K. & Jacobson, E. L. Endogenous UVA-photosensitizers: Mediators of skin photodamage and novel targets for skin photoprotection. *Photochem. Photobiol. Sci.* **5**, 215–237 (2006).
46. Golovynska, I., Golovynskyi, S. & Qu, J. Comparing the Impact of NIR, Visible and UV Light on ROS Upregulation via Photoacceptors of Mitochondrial Complexes in Normal, Immune and Cancer Cells. *Photochem. Photobiol.* (2022) doi:10.1111/php.13661.
47. Coates, D. R., Chin, J. M. & Chung, S. T. L. *Mitochondrial Oxidative Phosphorylation*.

Bone vol. 748 (Springer New York, 2012).
48. Schweitzer-Stenner, R. Cytochrome c: A Multifunctional Protein Combining Conformational Rigidity with Flexibility. *New J. Sci.* **2014**, 1–28 (2014).
49. Probes, M. S36002 Singlet Oxygen Sensor Green Reagent. 1–2 (2004).
50. Dąbrowski, J. M. *et al. Engineering of relevant photodynamic processes through structural modifications of metallotetrapyrrolic photosensitizers*. *Coordination Chemistry Reviews* vol. 325 (2016).
51. Arnaut, L. G. Design of porphyrin-based photosensitizers for photodynamic therapy. in *Inorganic Photochemistry* vol. 63 187–233 (Elsevier Inc., 2021).
52. Prasad, A., Sedlářová, M. & Pospíšil, P. Singlet oxygen imaging using fluorescent probe Singlet Oxygen Sensor Green in photosynthetic organisms. *Sci. Rep.* **8**, 1–13 (2018).
53. Atale, N., Gupta, S., Yadav, U. C. S. & Rani, V. Cell-death assessment by fluorescent and nonfluorescent cytosolic and nuclear staining techniques. *J. Microsc.* **255**, 7–19 (2014).
54. Brown, G. C. & Borutaite, V. Biochimica et Biophysica Acta Regulation of apoptosis by the redox state of cytochrome c. **1777**, 877–881 (2008).
55. Report, R., Kotlyar, A. B. & Borovok, N. Light-induced oxidation of cytochrome c. **1228**, 87–90 (1995).
56. Bombrun, A., Gerber, P., Casi, G., Terradillos, O. & Antonsson, B. 3,6-Dibromocarbazole Piperazine Derivatives of 2-Propanol as First Inhibitors of Cytochrome c Release via Bax Channel Modulation. *J Med Chem* **46**, 1–4 (2003).
57. Garner TP, Amgalan D, Reyna DE, Li S, Kitsis RN, G. E. Small Molecule Allosteric Inhibitors of BAX. *Nat Chem Biol.* (2019) doi:10.1038/s41589-018-0223-0.
58. Gomes-da-Silva, L. C. *et al.* Photodynamic therapy with redaporfin targets the endoplasmic reticulum and Golgi apparatus. *EMBO J.* **37**, (2018).